NASA Contractor Report 178373

ICASE REPORT NO. 87-62

ICASE

SPECTRAL COLLOCATION METHODS

M. Y. Hussaini

D. A. Kopriva

A. T. Patera

Contract No. NAS1-18107
September 1987

INSTITUTE FOR COMPUTER APPLICATIONS IN SCIENCE AND ENGINEERING
NASA Langley Research Center, Hampton, Virginia 23665

Operated by the Universities Space Research Association

National Aeronautics and
Space Administration

Langley Research Center
Hampton, Virginia 23665

SPECTRAL COLLOCATION METHODS

M. Y. Hussaini
Institute for Computer Applications in Science and Engineering
NASA Langley Research Center
Hampton, VA 23665

D. A. Kopriva
Department of Mathematics
Florida State University
Tallahassee, FL 32306

A. T. Patera
Mechanical Engineering Department
Massachusetts Institute of Technology
Cambridge, MA 02139

ABSTRACT

This review covers the theory and application of spectral collocation methods. Section 1 describes the fundamentals, and summarizes results pertaining to spectral approximations of functions. Some stability and convergence results are presented for simple elliptic, parabolic and hyperbolic equations. Applications of these methods to fluid dynamics problems are discussed in Section 2.

Research was supported by the National Aeronautics and Space Administration under NASA Contract No. NAS1-18107 while the authors were in residence at the Institute for Computer Applications in Science and Engineering (ICASE), NASA Langley Research Center, Hampton, VA 23665.

INTRODUCTION

Spectral collocation methods form an efficient and highly accurate class of techniques for the solution of nonlinear partial differential equations. They are characterized by the expansion of the solution in terms of global basis functions, where the expansion coefficients are computed so that the differential equation is satisfied exactly at a set of so-called collocation points. The fundamental unknowns are the solution values at these points. The expansion is used only for the purpose of approximating derivatives.

The popularity of these methods arises from several advantages which they have over common finite difference methods. First, they have the potential for rapidly convergent approximations. The dual representation in physical and transform space allows for automatic monitoring of the spectrum of a solution, providing thus a check on resolution. If certain symmetries exist in the solution, spectral methods allow the exploitation of these symmetries. Finally, the methods have low or non-existent phase and dissipation errors. For these reasons, spectral methods have become the primary solution technique in such areas of computational fluid dynamics as the simulation of turbulent flows and the computation of transition to turbulence. They are becoming increasingly viable in certain areas of computational aerodynamics such as compressible flows, boundary layers and heat transfer.

1.1 BASICS

The spectral representation of a function or solution to a differential equation is an expansion in a series of global orthogonal polynomials:

$$u(x) = \sum_{n=-\infty}^{\infty} a_n U_n(x). \tag{1}$$

If u is periodic, the usual basis (or expansion) functions, U_n, are complex exponentials, e^{inx}. If u is not periodic, Chebyshev or Legendre polynomials are often used. In general, expansions in terms of polynomials which are solutions of singular Sturm-Liouville problems are appropriate. This is discussed with regard to spectral solutions of a variety of boundary value problems in Gottlieb and Orszag [1] and in a more formal setting by Quarteroni [2]. Here we summarize the essential results for the one-dimensional case; the basis functions for multi-dimensions are defined by tensor products of one-dimensional basis functions.

The formally self-adjoint Sturm-Liouville eigenvalue equation is written as

$$LU_n \equiv \frac{1}{w}\left\{(pU_n')' + qU_n\right\} = \lambda_n U_n \qquad x\in[a,b] \tag{2}$$

where we assume that $p(x) > 0$ is differentiable and $q(x) \geq 0$ is continuous. The function $w(x) > 0$ is the weight function. It is well known (e.g., Courant and Hilbert [3]) that with the proper boundary conditions the eigenvalues of this equation form a countably infinite sequence. Also, the set of eigenfunctions $\{U_n\}$ is orthogonal and forms a basis for the Hilbert space L_w^2 with the weighted inner product

$$(u,v)_w = \int_a^b uvw\,dx \tag{3}$$

and norm $\|u\|_w = (u,u)_w^{1/2}$. Since the U_n are orthogonal, the coeffi-

cients a_n of equation (1) are defined by the relation $a_n = (u,U_n)_w/\|U_n\|_w$. By choosing $v = LU_n$ in equation (3), $u = U_n$ and integrating by parts,

$$a_n = \frac{1}{\lambda_n}(Lu,U_n)_w + \frac{1}{\lambda_n}[P(U_n'u - U_nu')]_a^b . \tag{4}$$

If the boundary conditions are periodic or if u and the U_n exactly satisfy homogeneous boundary conditions, then the second term is zero and

$$a_n = \frac{1}{\lambda_n}(Lu,U_n)_w. \tag{5}$$

From this point, Quarteroni [2] iterates to derive

$$a_n = \frac{1}{\lambda_n^m}(u_{(m)},U_n)_w \tag{6}$$

where $u_{(m)} = Lu_{(m-1)}$. From the properties of the λ_n, as $n\to\infty$,

$$|a_n| \leq \frac{C}{n^{2m}}\|u_{(m)}\|_w. \tag{7}$$

Thus, the magnitude of the coefficients of the expansion (1) depends only on the degree of smoothness of the solution. In particular, if u and the coefficients p and q are infinitely differentiable, then the a_n decay faster than any polynomial of $1/n$.

To ensure that inhomogeneous boundary conditions do not affect the rate of convergence for non-periodic problems, the second term of equation (4) must always be zero. This occurs if $p(x)$ is identically zero at the boundaries. The equation (2) is called a singular Sturm-Liouville equation if $p(x)$

$= 0$ at least at one of the boundaries. In general, one needs $p(x) = 0$ at both boundaries. The polynomials for which this is true are known as Jacobi polynomials. These polynomials are orthogonal with respect to the weight $w(x) = \alpha(1 - x)^{\sigma}(1 + x)^{\nu}$ and $p(x) = \beta(1 - x)^{\sigma+1}(1 + x)^{\nu+1}$ where $\alpha, \beta, \sigma, \nu$ are real constants. The most commonly used polynomials for spectral computations are the Chebyshev polynomials where $\sigma = \nu = -1/2$ and $\alpha = \beta = 1$ and the Legendre polynomials where $\sigma = \nu = 0$ and $\alpha = \beta = 1$.

In practice, the choice of basis depends on the type of boundary conditions and the efficiency with which the expansions can be computed. Fourier methods are certainly appropriate for problems with periodic boundary conditions. They can also be computed efficiently by using fast Fourier transform techniques (see Gottlieb and Orszag [1]). For non-periodic cases, Chebyshev spectral methods are popular because they can use a fast cosine transform. Legendre methods are not as commonly used because they lack a fast transform method.

1.2 COLLOCATION METHODS

The application of spectral methods consists of approximating the infinite sum in equation (1) with a finite sum by projecting the function onto a finite subspace of L^2_w. In particular, the collocation projection consists of finding the polynomial which takes on the exact value of the original function at a finite number of grid (or collocation) points. In other words, the collocation projection is interpolation. This method, often termed pseudo-spectral, is particularly useful for nonlinear problems.

1.2.1 FOURIER COLLOCATION

For problems with periodic boundary conditions, the Fourier expansion of a function $u(x)$ is given by the infinite series

$$u(x) = \sum_{k=-\infty}^{\infty} a_k e^{ikx}. \tag{8}$$

The collocation projection is defined by the discrete Fourier transform pair

$$P_N u = \sum_{k=-N/2}^{N/2-1} \hat{u}_K e^{ikx} \tag{9}$$

where the coefficients $\hat{u}_k$ are defined by

$$\hat{u}_k = \frac{1}{N} \sum_{j=0}^{N-1} u(x_j) e^{-ikx_j} \qquad k = \frac{-N}{2}, \frac{-N}{2}+1, \ldots, \frac{N}{2}-1. \tag{10}$$

The collocation points, x_j, are uniform on the interval $[0,2\pi]$

$$x_j = 2\pi j/N \qquad j = 0,1,2,\ldots N-1. \tag{11}$$

The transforms (9) and (10) are almost always computed by the use of a fast Fourier transform if N is a highly composite integer such as $N = 2^p 3^q$.

Derivatives of the function u at the collocation points are approximated by the derivatives of the interpolating polynomial. Thus, the ℓth derivative of u is approximated

$$\frac{d^\ell P_N u}{dx^\ell} = \sum_{k=-N/2}^{N/2-1} (ik)^\ell \hat{u}_k e^{ikx}. \tag{12}$$

From the form of equation (12), it is clear that the evaluation of the derivative at the collocation points can also be computed efficiently with a fast Fourier transform. See Hussaini, Streett, and Zang [4] for more information on the implementation of the Fourier collocation method.

1.2.2 CHEBYSHEV COLLOCATION

The collocation points for using a Chebyshev method to approximate a non-periodic function are usually defined by

$$x_j = -\cos(\pi j/N) \qquad j = 0,1,\ldots,N. \tag{13}$$

These points are the extrema of the N^{th} order Chebyshev polynomial, $T_N(x)$, and are obtained from the Gauss-Lobatto integration formula (see Davis and Rabbinowitz [5]).

The collocation projection operator is defined as the interpolation

$$P_N u = \sum_{n=0}^{N} a_n T_n(x) \tag{14}$$

where the coefficients are defined by

$$a_n = \frac{2}{N}\frac{1}{\bar{c}_n}\sum_{j=0}^{N}\frac{u(x_j)T_n(x_j)}{\bar{c}_j} \quad \text{where} \quad \bar{c}_j = \begin{cases} 2 & j = 1,N \\ 1 & \text{otherwise} \end{cases}. \tag{15}$$

Again, derivatives of u at the collocation points are approximated by the derivative of the interpolating polynomial evaluated at the collocation points. The first derivative, for example, is defined by

$$\frac{du}{dx} = \sum_{n=0}^{N} a_n^{(1)} T_n(x)$$

$$a_{N+1}^{(1)} = 0$$

$$a_N^{(1)} = 0 \tag{16}$$

$$\bar{c}_n a_n^{(1)} = a_{n+2}^{(1)} + 2(n+1)a_{n+1} \qquad n = N-1, 1, \ldots, 0 \ .$$

The transform pair given by equations (14) or (16) and (15) can be efficiently computed with a fast cosine transform. Equivalently, the interpolating polynomial and its derivatives can be computed using matrix multiplication. The matrices for the Chebyshev collocation method are conveniently collected in the review by Gottlieb, Hussaini, and Orszag [6]. For $N < 32$, this approach is competitive with using a fast cosine transform, at least on serial computers.

1.3 APPROXIMATION THEORY (COLLOCATION)

1.3.1 FOURIER COLLOCATION

The problem of how well $P_N u$ approximates u for Fourier approximations has been discussed by Kreiss and Oliger [7], Pasciak [8], and by Canuto and Quarteroni [9]. See also Mercier [10]. It is most convenient to express the interpolation results in terms of a Sobolev space, $H^m(0,2\pi)$. This is a Hilbert space with the norm

$$\|u\|_q = \sum_{j=0}^{q} |u|_j^2 \tag{17}$$

defined in terms of the seminorms

$$|u|_p^2 = \sum_{k=-\infty}^{\infty} k^{2p} |a_k|^2. \tag{18}$$

The use of the discrete Fourier transform pair (9), (10) represents the projection of the Sobolev space onto the space $S_N(0,2\pi)$, the space of Fourier polynomials of degree N.

The primary interpolation result is given by Theorem 1:

Theorem 1: *For any* $0 \leq p \leq q$ *with* $q > 1/2$ *there exists a constant* C *independent of* u *and* N *such that*

$$\|u - P_N u\|_p \leq C N^{p-q} |u|_q. \tag{19}$$

Proof: See Pasciak [8].

Equation (19) states that the rate of convergence depends (through the order of Sobolev norms) only on the smoothness of the function being approximated. This type of error decay is known as spectral accuracy. In practice, one sees errors which decay exponentially and hence spectral accuracy is often called exponential accuracy. Several applications described in Section 2 exhibit exponential accuracy. The term infinite order accuracy is also used often to refer to the case as $q \to \infty$.

Exponential accuracy has been shown explicitly by Tadmor [11] for functions u which are also analytic in the complex plane.

Theorem 2: Let u(x) be 2π-periodic and analytic in a strip of width $2s_0$. Then for any $0 < s < s_0$

$$\|u - P_N u\|_p \leq CM(s)/\sinh(s) N^p e^{-Ns} \tag{20}$$

where C depends on p and

$$M(s) = \max_{|\mathrm{Im} z| \leq s} |u(z)|.$$

Proof: See Tadmor [11].

If the solution is not very smooth, then the approximation may not be very good. In fact, if the function is discontinuous, the interpolant shows global oscillations (Gibbs phenomenon) and the approximation error decay is globally only first order. Smoothness is not usually a problem with the solutions of many elliptic or parabolic equations, but discontinuities are characteristic of the solutions of hyperbolic equations.

It is still possible to obtain spectrally accurate approximations to non-smooth functions, at least away from any discontinuities, but some type of filtering is required. Two papers which address this issue are Majda, MacDonough, and Osher [12] and Gottlieb and Tadmor [13]. The first approach used to smooth discontinuous solutions was that of Majda, MacDonough and Osher

[12] whose results show that spectral accuracy can be retained if Fourier space filtering is applied. Since the main results refer directly to the solutions of hyperbolic partial differential equations, they will be discussed in the next subsection.

Gottlieb and Tadmor [13] have taken the approach of smoothing in real space to allow the accuracy to depend on the local smoothness of the function. The smoothing procedure consists of convoluting the collocation approximation with a regularization kernel which is localized in space. If we call $\tilde{P}u$ the smoothed approximation to the originally oscillatory interpolant $P_N u$, the convolution takes on the form

$$\tilde{P}u(x) = 2\frac{\pi}{N}\sum_{j=0}^{N-1} P_N u(y_j)\psi^{\theta,p}(x - y_j) \tag{21}$$

where

$$\psi^{\theta,p}(y) = \frac{1}{2\pi\theta}\rho_\alpha\left(\frac{y}{\theta}\right)\frac{\sin((p+\frac{1}{2})\frac{y}{\theta})}{\sin(y/\theta)} \tag{22}$$

is the Dirichlet kernel localized in space by the cutoff function

$$\rho_\alpha = \begin{cases} e^{\alpha\xi^2/(\xi^2-1)} & |\xi| < 1 \\ 0 & \text{otherwise} \end{cases} . \tag{23}$$

The function ρ ensures that the kernel does not interact with any regions of discontinuity. For example, for a single discontinuity at $x = \pi$, they choose $\theta = \pi|x - \pi|$. With this smoothing, they show that the error depends only on the smoothness of the cutoff function $\rho(\xi)$:

Theorem: Let $\rho(\xi)$ be a C^{2s} cutoff function satisfying $\rho(0) = 1$ and having support in $[-\pi,\pi]$. Then for any x in $[0,2\pi]$ the smoothed function $\tilde{P}u$ satisfies the estimate

$$|\tilde{P}u(x) - u(x)| \leq C_s \|\rho\|_{2s} \underset{\substack{|y-x| \leq \theta\pi \\ 0 \leq k \leq 2s}}{\text{Max}} |D^k u(y)| (1 + \theta^{-2s}) N^{1-s} \qquad s > 1. \tag{24}$$

Proof: See Gottlieb and Tadmor [13].

1.3.2 CHEBYSHEV COLLOCATION

To study the approximation properties of the Chebyshev projection (14), it is practical to work in a weighted Sobolev space with weight $w(x) = (1 - x^2)^{-1/2}$. Defining the weighted L^2_w norm by

$$\|u\|^2_{0,w} = (u,u)_w = \int_{-1}^{1} u^2 w dx \tag{25}$$

and the Sobolev norm by

$$\|u\|^2_{q,w} = \sum_{i=1}^{q} \left\| \frac{d^i u}{dx^i} \right\|^2_{0,w} \tag{26}$$

the spectral approximation result is given by

Theorem 4: Let $q > 1/2$ and $0 \leq p \leq q$. Then there exists a constant C such that for all u in $H^q_w(-1,1)$

$$\|u - P_N u\|_{p,w} \leq CN^{2p-q} \|u\|_{q,w}. \tag{27}$$

Proof: See Canuto and Quarteroni [9].

So, like the Fourier approximation, the Chebyshev interpolation gives spectral accuracy; that is, the accuracy depends only on the smoothness of the function to be interpolated. Exponential convergence has also been proved by Tadmor [11]. This time, the function u must be analytic in an ellipse with foci at -1 and 1:

Theorem 5: Assume $u(x)$ is analytic in $[-1,1]$ and has a regularity ellipse whose sum of its semi-axes equals $r_0 = \exp(\eta_0) > 1$. Then for any $\eta, 0 < \eta < \eta_0$ we have

$$\|u(x) - P_N u\|_{H_T^1} \leq 8M(\eta)\left(\frac{\coth(N\eta)}{e^{2\eta} - 1}\right)^{1/2} Ne^{-N\eta} \tag{28}$$

where the norm is defined by

$$\|u\|_{H_T^1} = \sum_{p=0}^{\infty} (1+p)^2 |\hat{u}_p|^2. \tag{29}$$

Proof: See Tadmor [11].

If the function which is being approximated is discontinuous, it is still theoretically possible to recover a spectrally accurate solution [13] by filtering in physical space. The procedure is the same as the smoothing proce-

dure for the Fourier case, but the Dirichlet kernel is replaced by

$$K_p(y) = \frac{(1 - y^2)}{p\pi} \frac{T_p'(y)}{y} . \tag{30}$$

1.4 THEORY OF SPECTRAL COLLOCATION METHODS FOR PDE'S

Proofs of the convergence of spectral approximations to partial differential equations are usually accomplished using energy methods which mimic proofs of the well-posedness of the original equations. Consequently, it is most convenient to discuss stability and convergence with respect to the three major types of partial differential equations separately.

1.4.1 ELLIPTIC EQUATIONS

Theoretical analysis of the convergence of Fourier collocation methods is simplified because of periodic boundary conditions. The elliptic problem is to find the function $u(x)$ which satisfies

$$\begin{aligned} &Lu = f \qquad x\epsilon[0,2\pi] \\ &u(0)=u(2\pi) \end{aligned} \tag{31}$$

where L has the property

$$(Lu,u) \geq \alpha \|u\|_1^2 \quad \alpha > 0. \tag{32}$$

The Fourier collocation approximation is obtained as described in section

1.2.1 and satisfies the same inequality, i.e., $\forall u \in S_N$

$$(L_c u, u) \geq \alpha \|u\|_1^2.$$

Then we have the

Theorem 6: For $\tau > 1$ there exists a constant C such that if $f \in H_p^{\tau-2}(0,2\pi)$ and $u \in H_p^{\tau}(0,2\pi)$ then the following estimate is optimal:

$$\|u - P_N u\|_1 \leq C(1 + N^2)^{(1-\tau)/2} \|u\|_\tau. \tag{33}$$

Proof: See Mercier [10].

Chebyshev methods with both Dirichlet and Neumann boundary conditions have been analyzed for the elliptic differential equation of the form

$$Lu = -(au_x)_x + (bu)_x. \tag{34}$$

The Chebyshev spectral collocation approximation is formally written as

$$L_c u_c = -\frac{d}{dx}\left(P_N\left(a \frac{d}{dx} u_c\right)\right) + \frac{dP_N(bu_c)}{dx} + \gamma u_c. \tag{35}$$

For Dirichlet problems, the equation is collocated at the interior points and boundary conditions of the form

$$u(-1) = u_l \quad \text{and} \quad u(+1) = u_r \tag{36}$$

are specified directly at the boundary points. Stability and convergence were proved by Canuto and Quarteroni [14] using a variational approach. They show

Theorem 7: Let u_c be the solution to $L_c u_c = f_c$ where L_c is defined by equation (35) with homogeneous boundary conditions, $u_r = u_l = 0$ then with suitable conditions on a, b, α the following estimate holds

$$\|u - u_c\|_{1,w} \leq C_1 N^{1-r} \|u\|_{r,w} + C_2 N^{-s} \|f\|_{s,w}. \tag{37}$$

Proof: See Canuto and Quarteroni [14], Theorem 2.4.

Convergence proofs for Neumann or mixed-type boundary conditions are available for boundary conditions applied in one of two different ways. A discussion of these approaches can be found in Canuto [15], [16]. The first approach is explicit. At interior points, the equation is collocated normally as in equation (35). At the boundary points, however, the collocation approximation to the derivative is written in matrix form and the boundary conditions are used to determine the value at the boundary point. Thus, the approximation to the boundary condition

$$\begin{aligned} B_l u &= \beta u_x + \alpha u \\ B_r u &= \delta u_x + \gamma u \end{aligned} \tag{38}$$

is found by solving the system

$$(\alpha + \beta d_{00})u_0 + \beta d_{0N}u_N = -\beta \sum_{j=1}^{N-1} d_{0j}u_j$$
$$(\gamma + \delta d_{NN})u_N + d_{N0}u_0 = -\delta \sum_{j=1}^{N-1} d_{Nj}u_j \tag{39}$$

where $u_j = u_c(x_j)$ and $[d_{ij}]$ is the matrix for the derivative at the collocation points (see Gottlieb, Hussaini, and Orszag [6]).

The convergence is very rapid for smooth solutions:

Theorem 8: Let $\sigma > 1/2$ and let u and u_c be solutions to $Lu = f$ and $L_c u_c = f_c$ where L and L_c are defined as above. Then with explicitly applied Neumann boundary conditions the following convergence estimate holds

$$\|u - u_c\|_{2,\eta} \leq CN^{-\sigma}\{\|u\|_{\sigma+2,w} + \|f\|_{\sigma,w}\} \tag{40}$$

where $\eta = (1 - x^2)w(x)$ and C is independent of N.

Proof: See Canuto and Quarteroni [14], Theorem 3.2.

Canuto [16] also describes how to impose Neumann boundary conditions implicitly for elliptic problems. In this way, the boundary conditions are not exactly satisfied because what is actually solved is the modification of the interior approximation. For the spectral case of a pure Neumann problem, the first derivatives are computed normally as in equation (16). At the boundary points, the derivatives are replaced by the Neumann conditions. Then the second spectral derivatives are computed by using (16) again on the modi-

fied set of derivatives. This has the advantage that all of the points are treated the same, but the boundary conditions are not exactly satisfied. The boundary error does decay spectrally, however.

Theorem 9: Let u_c be the solution to $L_c u_c = f$ with implicit Neumann boundary conditions. If $u \in H_w^m(-1,1)$ with $m > 5/2$ then

$$\left|\frac{\partial u_c}{\partial x}(\pm 1)\right| \leq C N^{4-m} \|u\|_{m,w} \tag{41}$$

where $C > 0$ is independent of N.

Proof: See Canuto [16].

The convergence in the interior is also spectral, and the estimate bounds both the solution and the collocation derivative.

Theorem 10: Under the assumptions of Theorem 9,

$$\|u - u_c\|_{0,w} + \left(\sum_{j=1}^{N-1} [u_x - (u_c)_x](x_j) w_j\right)^{1/2} \leq C N^{2-m} \|u\|_{m,w} \tag{42}$$

where the w_j are the Gauss-Lobatto weights at the points x_j.

Proof: See Canuto [16].

1.4.2 PARABOLIC EQUATIONS

The convergence and stability theory for linear parabolic equations, like the theory for elliptic equations, is fairly well developed. In particular, the theory has centered on studies of semi-discrete equations in which the spatial variation is discretized, but the time variation is left continuous. The emphasis, however, has been on application to boundary value problems--that is, on the convergence of Chebyshev collocation methods. In this section we survey theoretical results for initial-value problems of the form

$$u_t = (Au_x)_x + Bu_x + Cu + f$$
$$u(x,0) = u_0(x) \tag{43}$$

where A, B, and C are n x n matries. The general collocation approximation to the first, third, and fourth terms of the right hand side of equation (43) is written in a manner identical to that of the elliptic equations in equation (35).

Stability of the Fourier approximation of the heat equation is easy to prove and is discussed in Gottlieb, Hussaini, and Orszag [6]. The more complicated case is equation (43) above. Kreiss and Oliger [17] have proved stability with two different treatments of the first order term. The first treats it in "skew symmetric form", that is, by writing

$$Bu_x + Cu = \frac{1}{2}(Bu_x + (Bu)_x) + (C - \frac{1}{2}B_x)u. \tag{44}$$

The second, discussed more fully in the next section, involves filtering the

first derivative to ensure stability. A convergence estimate using the skew symmetric form for the scalar equation with $f = 0$ is

Theorem 11: Let $\tau \geq 1$, $T > 0$, and assume that $u_0 \in H_p^{\tau+1}(0,2\pi)$. Then there exists a constant C such that the following estimate holds:

$$\|u(t) - u_c\|_0 \leq C(1 + N^2)^{(1-\tau)/2}\{\|u_0\|_{\tau-1} + [\|u_0\|_\tau^2 + (\|u_0\|_\tau + \|u_0\|_{\tau+1})^2]^{1/2}\} \quad (45)$$

for all $t \in [0,T]$.

Proof: See Mercier [10] Theorem 11.2. Here H_p is defined in terms of distribution derivatives of periodic functions.

The convergence of Chebyshev approximations to parabolic equations on bounded domains has received a lot of attention recently. The spatial approximation for a Dirichlet problem will be exactly like that for the elliptic problem. Stability for the heat equation with non-constant coefficients was originally shown by Gottlieb [18]. Convergence estimates were worked out by Canuto and Quarteroni [19]. For the scalar heat equation

$$u_t = a(x)u_{xx} \qquad x \in (-1,1) \quad (46)$$

with homogeneous boundary conditions $u(-1,t) = u(1,t) = 0$ they show

Theorem 12: Let $\sigma > 1/2$ and $S > \sigma + 2$ and $T > 0$. If $u \in L^1(0,T; H_w^S(-1,1))$ then there is a constant C, independent of N such

that

$$\|u(t) - u_c(t)\|_N \leq C\ N^{2\sigma+4-S} \tag{47}$$

where the norm $\|\cdot\|_N$ is the discrete norm derived from the Gauss-Lobatto integration formula

$$\|v\|_N = \sum_{j=0}^{N} \frac{w_j v(x_j)^2}{a(x_j)} . \tag{48}$$

Neumann boundary conditions for parabolic problems can also be applied either explicitly or implicitly. For the implicit treatment, convergence is similar to that of the corresponding elliptic equation:

Theorem 13: Suppose the solution to the differential equation (46) with Neumann boundary conditions is regular to the extent that $u \in L^2(0,T;H_w^m(-1,1))$ and the time derivative satisfies $u_t \in L^2(0,T;H_w^{m-1}(-1,1))$ for $T > 0$ and $m > 5/2$. If $u_0 \in H_w^m(-1,1)$ then

$$\|u(t) - u_c(t)\|_{0,w} + \left[\sum_{j=1}^{N-1} (u_x - (u_i)_x)^2 w_j\right]^{1/2}$$

$$\leq C_1 N^{2-m}\{\|u_0\|_{m,w} + e^{t/2}\left[\int_0^t \|u\|_m^2 d\tau\right. \tag{49}$$

$$\left. + \int_0^t \|u_t(\tau)\|_{m-1}^2 dt\right\}.$$

Proof: See Canuto [16] Theorem 4.4.

1.4.3 HYPERBOLIC EQUATIONS

The study of the convergence of spectral approximations to hyperbolic equations is complicated by the fact that the straight-forward discretization of an equation of the form

$$u_t + a(x)u_x + bu = 0 \tag{50}$$

written as

$$\frac{\partial u_c}{\partial t} + P_N(a(x)\frac{\partial u_c}{\partial x}) + bu_c = 0 \tag{51}$$

is often unstable. In this section, we will discuss the available theory of formally stable approximations.

Fourier methods are stable if $a(x)$ is of fixed sign. If $a(x)$ in equation (50) is strictly positive and $b = 0$, the energy estimate for the approximation, (51)

$$\frac{d}{dt}\sum_{j=0}^{N-1}\frac{u_c^2(x_j)}{a(x)_j} = 0 \tag{52}$$

shows that the approximation is stable. If $a(x)$ is zero at some point, however, then this estimate is not valid and no general technique is available to show stability.

Two basic approaches have been used to devise schemes which can be shown to be stable. The first, indicated in the last section, is to write the spatial derivative in skew-symmetric form. That is, instead of computing (51), one computes

$$\frac{\partial u_c}{\partial t} + 1/2\ P_N\{\frac{a\partial u_c}{\partial x} + \frac{\partial (P_N a u_c)}{\partial x}\} - 1/2\ P_N\{\frac{u\partial a}{\partial x}\} + bu_c = 0. \tag{53}$$

Kreiss and Oliger [20], [17] showed that this discretization is stable. Mercier [10] examined the stability and convergence of the Fourier approximation to the skew-symmetric equation

$$u_t + v(x)u_x + (v(x)u)_x = 0 \tag{54}$$

and showed that the error decay is spectral.

Theorem 14: For $\tau > 1$ and $T > 0$, if the initial condition satisfies $u(x,0) \in H_p^{\tau}(0,2\pi)$ then there is a constant C independent of N such that

$$\|u(t) - u_c(t)\| \leq C(1 + N^2)^{(1-\tau)/2}\|u_0\|_{\tau}. \tag{55}$$

Proof: See Mercier [10], Theorem 9.1.

Though approximations written in skew symmetric form are stable, there are objections to their use. The first objection is that they are less efficient since they have twice as many derivatives to evaluate. More important, conservation is lost when this is applied to conservation law equations (such as the equations of gas-dynamics) for the computation of weak solutions. Tadmor [21] has examined the skew-self adjoint form of systems of non-linear conservation laws. They can be explicitly shown to be well-posed, but the conservation property is lost.

The alternative to rewriting the equation in skew-symmetric form is to use the approximation of equation (51) and filter the solutions. Finite

difference solutions are often filtered by adding an explicit low order artificial viscosity. The goal of filtering Fourier spectral solutions is to do so without destroying the accuracy of the method.

Two approaches for filtering Fourier approximations to guarantee stability have been suggested. The first was proposed by Majda, McDonough and Osher [12]. In their method, the spectral derivative defined in equation (12) is modified by filtering the computed solution. For linear problems, this can be done efficiently by modifying the Fourier coefficients of the solution and using those new coefficients when the derivative is computed. Let $\rho(x) \in c^{\infty}(-\pi,\pi)$ be a "filter function". Its values are zero near $\theta = \pm \pi$ and identically one in a neighborhood of $\theta = 0$. The Fourier coefficient $\hat{u}_k$ is replaced by $\rho(2\pi k/N)\hat{u}_k$ and this is used in equation (12) to compute the derivative.

For smooth initial conditions, smoothing gives a stable approximation and spectral accuracy

Theorem 15: *For* $u_0 \in C^{\infty}$ *the error satisfies the inequality*

$$\| u(x,t) - u_c(x,t) \|_s \leq C\, h^{\lambda} \quad \text{for all } s,\lambda \tag{56}$$

where C *depends on both* s *and* λ.

Proof: See Majda, McDonough, and Osher [12], Corollary 1.

If the solution is discontinuous, it is still possible to obtain spectral accuracy in the sense of equation (56) if the initial condition is properly

smoothed. It is not enough to smooth the discrete Fourier coefficients of the initial condition with a filter whose support is enclosed within the support of ρ. Rather, it is necessary to use smoothed versions of the exact Fourier coefficients.

A different approach to filtering was proposed by Kreiss and Oliger [17]. Instead of filtering the solution with a predefined filter, they showed that linear stability could be obtained by smoothing the space derivative with a weak filter which depends on the smoothness of the function. They arbitrarily split the frequency range of the solution into a high frequency range, $|k| > N_1$, and a low frequency range, $|k| \leq N_1$. The coefficients of the low frequency range are not modified at all. The coefficients of the high frequency range are modified only if they do not decay rapidly enough. Call $v(x) = u_x$ defined by equation (12) and define v_1 to be the derivative summing only the low frequency components $|k| \leq N_1$. The modified coefficients of the derivative are defined to be $w = Hv$ where

$$w_k = \begin{cases} v_k & \text{for } |k| \leq N_1 \\ v_k & \text{if } |k| > N_1 \text{ and } |v_k| \leq D \|v_1\|/|k|^j \\ D \|v_1\| v_k/(|v_k|\ |k|^j) & \text{otherwise.} \end{cases} \tag{57}$$

Kreiss and Oliger prove the following stability theorem:

Theorem 16: Suppose the coefficient $a(x)$ in equation (50) is smooth so that its Fourier coefficients decay at a rate $|k|^{-\beta}$. The approximation

$$u_t + P_N(a \frac{H\partial u_c}{\partial x}) = 0 \tag{58}$$

where the filter H is defined by (57) is stable and converges if $j = \beta > 2$.

Proof: See Kreiss and Oliger [17], Theorem 4.2.

For linear problems, however, it is not clear that filtering is always needed. The fact that the energy method gives only a sufficient condition for stability means that equation (52) does not prove instability if a is not of one sign. For example, Gottlieb, Orszag, and Turkel [22] show stability in the usual sense of convergence as $N \to \infty$ of the scalar equation where $a(x) = A\sin(x) + B\cos(x) + C$ for arbitrary A, B, C. The numerical solutions do, however, grow in time - just as the exact solutions do.

For non-linear problems, experience shows that filtering of the Fourier approximation is needed, particularly if there are discontinuities in the solutions. Hussaini, Kopriva, Salas, and Zang [51] discuss the application of these filtering methods and the choice of filters to a periodic transonic flow with a shock.

Proofs of the stability and convergence of Chebyshev approximations have the added complication of the boundary conditions and the weight, $w(x)$, which is unbounded at the endpoints. In particular, the case where $a(x)$ changes sign makes it difficult to show stability. Gottlieb [18] has proved stability of the straightforward Chebyshev collocation for the special cases where $a(x) = \pm x$.

To show stability of Chebyshev approximations in general, the skew-symmetric form of the equations is needed. We will survey the convergence theory of Canuto and Quarteroni [23] for the special case of the hyperbolic boundary value problem with $b(-1) > 0$

$$
\begin{aligned}
& u_t + (bu)_x + b_0 u = f && x\in(-1,1), \quad t\in(0,T] \\
& u(-1,t) = 0 && t\in(0,T] \\
& u(x,0) = u_0 && x\in(-1,1).
\end{aligned} \tag{59}
$$

The further assumtion is added that

$$
1/2\ b_x + b_o - 1/2\ bw_x w^{-1} \geq 0 \qquad \text{for} \quad x\in(-1,1). \tag{60}
$$

For the Chebyshev weight $w(x) = (1 - x^2)^{-1/2}$, the use of integration by parts to get an energy estimate will give an unbounded boundary term evaluated at $x = +1$ (see Gottlieb and Orszag [1]). This has led to the use of a modified weight and norm with which to prove stability and convergence. Let the new weight be $w^*(x) = (1 - x)w(x)$ so that $w^*(1) = 0$. Then the following convergence estimate holds:

Theorem 17: Suppose that $u\in L^\infty(0,T;\ H^\beta_{w^*}(-1,1))$ and $b \in H^\beta_{w^*}(-1,1)$ for $\beta > 2$. Then the skew-symmetric Chebyshev approximation to (59) satisfies

$$
\| u - u_c \|_{L^\infty(L^2_{w^*})} \leq CN^{2-\beta} \| u \|_{L^\infty(H^\beta_{w^*})}. \tag{61}
$$

Proof: See Canuto and Quarteroni [23], Theorem 2.3. Note: Their theorem actually allows for more general boundary conditions than we have mentioned here.

For computations which are not done in skew-symmetric form, such convergence estimates are not available in the general case. As indicated above, Gottlieb [18] has shown stability in some particular cases. However, Reyna [24] has shown that if $b(x)$ is not strictly positive in the interval that a straight-forward Chebyshev approximation need not be stable. To stabilize the solutions he proposes the use of filtering. It is not sufficient, however, to simply smooth the Chebyshev coefficients. Rather, he shows that stability can be proved if Legendre coefficients are computed from the Chebyshev ones, the Legendre coefficients are smoothed, and then transformed back.

The stability and convergence of Chebyshev approximations to the hyperbolic initial-boundary-value problem for systems

$$u_t = Au_x \qquad -1 \leq x \leq 1, \quad t \geq 0 \tag{62}$$

where u is an n-vector and A is a constant matrix has recently been proved by Gottlieb, Lustman, and Tadmor [25], [26]. Because this system is hyperbolic, the matrix A can be assumed to have been diagonalized to

$$A = \begin{bmatrix} A^I & 0 \\ 0 & A^{II} \end{bmatrix}$$

where $A^I < 0$, $A^{II} > 0$ are diagonal matrices.

Boundary conditions for which this system is well posed are of the form

$$\begin{aligned} u^I(-1,t) &= Lu^{II}(-1,t) + g^I(t) \\ u^{II}(1,t) &= R\, u^I(1,t) + g^{II}(t) \end{aligned} \tag{63}$$

where u^I and u^{II} represent the partition of u into inflow and outflow components (see Kreiss and Oliger [5]). Under the assumption that the boundary conditions are dissipative, the standard Chebyshev collocation is stable:

Theorem 16: *Under the assumption that* $|R| \cdot |L| \leq 1 - \delta < 1$, *the Chebyshev collocation method is stable for the system (62) with boundary conditions (63) in the sense that there exists a weighting pair* $w(x)$ *and constants* q *and* $\eta_0 \geq 0$ *such that for all* s *with* $\mathrm{Re}\, s = \eta > \eta_0$

$$(\eta - \eta_0)\|\hat{u}_c(x,s)\|^2 \leq CN^{2q}|\hat{g}(s)|^2$$

where $\hat{u}_c$ *and* $\hat{g}$ *are the Fourier transforms of* u_c *and* g.

Proof: See Gottlieb, Lustman, and Tadmor [25].

2. SOME APPLICATIONS OF SPECTRAL COLLOCATION METHODS

In this section, some recent developments in the application of spectral methods to problems in fluid mechanics are surveyed. Much current emphasis has involved making spectral methods more efficient and more applicable to problems with complicated geometries. This has lead to the development of spectral multidomain methods which eliminate the need for global mappings and to the development of iterative techniques for the rapid inversion of the full matrices which occur when implicit time discretizations are used.

2.1. METHODS FOR ELLIPTIC AND PARABOLIC PROBLEMS

2.1.1. SPECTRAL MULTIDOMAIN METHODS

Spectral multidomain methods have been developed in order to avoid the need for global mappings required by spectral methods in problems with complicated geometries. A complicated domain can be subdivided into several subdomains and individual spectral discretizations can be applied to each subdomain. For elliptic and parabolic problems, for handling the interfaces, early work considered explicit enforcement of continuity (e.g. Orszag [27] and Morchoisne [28]). More recently, spectral element discretizations and enforcement of global flux balance have been used. The spectral element methods retain the accuracy of spectral methods in the context of a geometrically flexible finite element formulation. Global flux conservation has been used effectively when the mappings and/or domain sizes vary radically across interfaces.

Consider first the solution of the (second-order, self-adjoint, elliptic) Helmholtz equation,

$$\nabla^2 u - \lambda^2 u = f \quad \text{in} \quad D \tag{64}$$

with Dirichlet boundary conditions on the domain boundary, ∂D. Following the lead of finite element techniques, the spectral element algorithm [29, 30] proceeds by recognizing the equivalence of (64) to maximization of the following variational form,

$$\max_{u \in H^1} \int_D \{-\nabla u \cdot \nabla u/2 - \lambda^2 u^2/2 - uf\} dx, \tag{65}$$

The variational form, (65), is preferable over the differential statement, (64), in that it requires less continuity of candidate solutions.

The spectral element discretization proceeds by breaking up the computational domain, D, into general quadrilateral elements. Within a given element k, the solution, geometry, and data are then expanded as tensor product Lagrangian interpolants through a set of specified collocation points. For instance, in two space dimensions, the solution u in element k is represented as,

$$u^k(r,s) = \sum_i \sum_j u^k_{ij} h_i(r) h_j(s) \tag{66a}$$

$$h_m(z_n) = \delta_{mm}, \tag{66b}$$

where r and s are the local elemental coordinates, the h_i are the Lagrangian interpolants, the z_n are the collocation points, and δ_{mm} is the Kronecker delta symbol. All summations run from 0 to N, where N is the order of the Lagrangian interpolants in each element.

The expansions (66a) are then inserted into (65), and the functional rendered stationary with respect to arbitrary variations in the nodal values, u^k_{ij}. Direct stiffness summation [31] (which recognizes that the global approximation space must be C^0) is then used to assemble the elemental equations into the system matrix. It should be noted that, as regards the treatment of elliptic and parabolic equations, the "spectral element" recipe presented here is very similar to earlier "p-type finite element" methods [32] and the "global element" method [33].

It is clear from the above representation, (66), that the global interpolant space is only C^0, that is, that the approximation space suffers dis-

continuities in derivative at elemental boundaries. Although this may appear to violate the basic smoothness required of spectral methods, this is not the case due to the fact that the variational formulation, (65), is used rather than the (unintegrated) Galerkin weighted-residual form. In particular, in the absence of "variational crimes", the spectral element method can be shown to achieve exponential convergence to smooth solutions as N, the order of (fixed) elements, is increased. For nonsmooth solutions (e.g., corner-induced singularities), high-order convergence is more difficult to obtain, however refinement techniques have been developed for the p-type finite element method [32].

Variational crimes take the form of numerical quadrature errors and interpolation of boundary data. (Nonconforming elements are not considered.) In order to insure that these errors do not dominate the approximation errors, it is important to correctly choose the collocation points of the Lagrangian interpolants. Earlier work on spectral elements used the Chebyshev collocation points, as they are simple to evaluate and amenable to fast transform techniques. However, as the variational formulation (65) has essentially a unity weighting, it appears that a better choice is the Legendre-Lobatto points from the point of view of accuracy and efficiency of numerical quadratures [6, 34]. Although Legendre polynomials are less convenient than Chebyshev polynomials, are subject to round-off errors for high-order expansions, and cannot be "fast transformed", none of these objections are particularly oppressive for the relatively low-order expansions used in spectral element methods.

As an example of the accuracy of a Legendre spectral element [34] (see [29, 30] for extensive discussion of Chebyshev-based techniques), consider the

problem

$$\nabla^2 u = 0 \qquad \text{in} \quad D \tag{67a}$$

where D is the domain defined in Figure 1, $x\in[0, 1]$, $y\in[0, 1 + \frac{1}{2}\sin\pi x]$. Dirichlet boundary conditions are imposed such that the solution to the problem is given by,

$$u(x,y) = \sin(x)e^{-y}. \tag{67b}$$

The L_∞ error for the spectral element mesh shown in Figure 1 is plotted in Figure 2. As expected from the analytic nature of the solution (67b) in the complex plane, exponential convergence is achieved as the order of the elements is increased.

As another example of elliptic problems, consider the moving-boundary Stefan problem [34], given by

$$\nabla^2\theta = 0 \qquad \text{in} \quad D_1, D_2 \tag{68a}$$

$$\theta = 1/2 \quad \text{on} \quad \partial D_I \tag{68b}$$

$$\nabla\theta\cdot\hat{n}\big|_- + 3\nabla\theta\cdot\hat{n}\big|_+ = 0 \quad \text{on} \quad \partial D_I \tag{68c}$$

$$\nabla\theta\cdot\hat{n} = 0 \quad \text{on} \quad \partial D_0 \tag{68d}$$

$$\theta = 1 + 1/2\cos 2\pi x \quad \text{on} \quad \partial D_1 \tag{68e}$$

$$\theta = 0 \quad \text{on} \quad \partial D_2, \tag{68f}$$

where D_1, D_2, ∂D_I, ∂D_0, ∂D_1, and ∂D_2 are defined in Figure 3. Here the evaluation of $_-$ and $_+$ refer to the D_1 and D_2 sides of ∂D_I, respectively. In point of fact, the time-dependent (parabolic) version of (68) was solved, approaching the steady-state only as $t \to \infty$; since the solution of parabolic equations involves at each time step the solution of an elliptic equation of the form (64), this aspect of the problem does not warrant separate discussion.

Solution of the Stefan problem (68) illustrates several aspects of the spectral element method. First, since the interface ∂D_I is unknown and general, it demonstrates the ability to handle complex geometry. Second, though the solution suffers a discontinuity at ∂D_I the method has the ability to resolve certain non-homogeneities without losing "spectral accuracy". Figure 4 shows the interface position obtained with a Legendre spectral element method using a two-element mesh. In Figure 5, the associated temperature (θ) distribution is given. High accuracy can be achieved with very few points.

It is critical that the spectral element schemes not only be accurate, but also efficient as regards work required for a given level of accuracy. The key to the computational efficiency of the techniques is the sum factorization which follows from the tensor product representation, (66). For instance, a typical elemental term in a two-dimensional Chebyshev spectral element equation is of the form,

$$\sum_m \sum_n \int h_i h_m \, dr \int h_j h_n \, ds \, u_{mn} \tag{69}$$

where h_i, u_{mn} are defined as in (66), and all subscripts range from 0 to

N, the order of the polynomial space in each co-ordinate direction. Naive evaluation of this sum gives an operation count of $O(N^3)$, and $O(N^4)$ in three dimensions. This sum factorization is at the heart of both direct solvers using static condensation and fast eigenfunction solvers [35] and iterative solvers using conjugate gradient algorithms [36].

Another approach to handling domain interfaces was taken by Macaraeg and Streett [37], [38]. Within subdomains, the usual collocation procedure described in Section 1.2.2 is used. The interface values are computed by requiring that the solution be continuous and that the global flux be balanced. As an example of the procedure, consider the equation

$$\begin{aligned} G(u) \equiv F_x(u) - vu_{xx} &= S(u) \\ u(-1) &= a \\ u(1) &= b \end{aligned} \tag{70}$$

where an interface is placed at $x = x_i$. Integration of (70) from -1 to 1 and the requirement that the jump in the flux [G] be zero at the interface yields

$$G(u)_{x=-1} + \int_{-1}^{x_i} S(u)dx = \bar{G}(u)_{x=1} - \int_{x_i}^{1} S(u)dx. \tag{71}$$

Numerical experiments show that spectral accuracy is retained. In two dimensions, the method has been used to solve Laplace's equation with discontinuous boundary conditions.

2.1.2 ITERATIVE SPECTRAL METHODS

For evolution problems, explicit time-stepping can be extremely inefficient. This is because the typical time-step limitation for spectral methods is proportional to $1/N^2$ for the advection equation and $1/N^4$ for the diffusion equation (where N is the number of modes) [39]. Hence, implicit time-stepping becomes a necessity. This results in a set of algebraic equations which are, in general, amenable to iterative solution techniques only. Also, elliptic equations governing practical problems virtually require implicit iterative techniques. Since the condition number of the relevant matrices are large, preconditioned iterative schemes including multigrid procedures are the attractive choices. In this section, the fundamentals of iterative spectral methods are discussed with reference to an elementary example.

For the purpose of illustration, consider the equation,

$$u_x = f, \tag{72}$$

periodic on $[0,2\pi]$. For the Fourier method, the standard choice of collocation points is given in Equation (11).

The Fourier collocation discretization of the equation (72) may be written

$$LU = F, \tag{73}$$

where $U = (u_0, u_1, \ldots, u_{N-1})$, $F = (f_0, f_1, \ldots, f_{N-1})$, and $L = C^{-1}DC$. Here C is the discrete Fourier transform operator, C^{-1} the inverse transform, and D the diagonal matrix denoting the first derivative operator in the Fourier space. Specifically,

$$C_{jk} = e^{-2\pi i k \frac{(j-N/2)}{N}}, \qquad j,k = 0, 1, \ldots, N-1$$

and (74)

$$d_{jj} = \begin{cases} i(j - N/2) & \text{for } j = 1,2, \ldots, N-1 \\ = 0 & \text{for } j = 0 \end{cases}$$

The eigenvalues of L are $\lambda(p) = ip$, $p = -N/2 + 1, \ldots, N/2 - 1$, and the largest one grows as $N/2$. A preconditioned Richardson iterative procedure for solving Eq. (73) is

$$V \leftarrow V + \omega H^{-1} (F - LV) \tag{75}$$

where the preconditioning matrix, H, is a sparse, readily invertible approximation to L. An obvious choice for H is a finite difference approximation L_{FD} to the first derivative. With the various possibilities for L_{FD}, the eigenvalue spectrum of $L_{FD}^{-1}L$ is given in Table I. Apparently, the staggered grid leads to the most effective treatment of the first derivative. This kind of preconditioning was successfully used in the semi-implicit time-stepping algorithm for the Navier-Stokes equations discussed in section 2.2 on Navier-Stokes Algorithms. The eigenvalue trends of that complicated set of vector equations are surprisingly well predicted by this extremely simple scalar periodic problem.

Next, consider the second order equation

$$-u_{xx} = f \qquad \text{on } [0,2\pi] \tag{76}$$

with periodic boundary conditions. A Fourier collocation discretization of

this equation is the same as Eq. (73) except for the diagonal matrix D which represents now the second derivative operator in the Fourier space.

$$D_{jj} = \begin{cases} -(j - \frac{N}{2})^2, & j = 1, 2, \ldots, N-1 \\ 0, & j = 0 \end{cases} . \tag{77}$$

The eigenvalues of L are $\lambda(p) = p^2$, $p = -N/2 + 1, \ldots, N/2-1$. To make the case for the multigrid procedure (consisting of a fine-grid operator and a coarse-grid correction) as a preconditioner, assume H to be the identity matrix I in the iterative scheme (75). The iterative scheme is convergent if the eigenvalues, $(1 - \omega\lambda)$, of the iteration matrix $[I - \omega L]$ satisfy

$$|1 - \omega\lambda| < 1.$$

Each iteration damps the error component corresponding to λ by a factor $v(\lambda) = |1-\omega\lambda|$. The optimal choice of λ is that which balances damping of the lowest-frequency and the highest-frequency errors, i.e.,

$$(1 - \omega\lambda_{max}) = -(1 - \omega\lambda_{min}) \tag{78}$$

This yields

$$\omega_{SG} = \frac{2}{(\lambda_{max} + \lambda_{min})} , \tag{79}$$

and the spectral radius

$$\mu_{SG} = \frac{(\lambda_{max} - \lambda_{min})}{(\lambda_{max} + \lambda_{min})} . \tag{80}$$

In the present instance, $\lambda_{max} = N^2/4$, $\lambda_{min} = 1$, and thus $\mu_{SG} = 1 - 8/N^2$.

This implies order N^2 iterations are needed for convergence. This poor performance is due to balancing the damping of the lowest frequency eigenfunction with the highest-frequency one. The multigrid procedure exploits the fact that the lowest-frequency modes ($|p| < N/4$) can be damped efficiently on coarser grids, and settles for a relaxation parameter value which balances the damping of the mid-frequency mode ($|p| = N/4$) with the highest-frequency one ($|p| = N/2$). Table II provides the comparison of single-grid and multigrid damping factors for N=64. The high frequencies from 16 to 32 are damped effectively in the multigrid procedure, whereas the frequencies lower than 16 are hardly damped at all. But then some of these low frequencies (from 8 to 16) can be efficiently damped on the coarser grid with N=32. Further coarser grids can be employed until relaxation becomes so cheap that all the remaining modes can be damped. In concrete terms, the ingredients of a multigrid technique are a fine-grid operator, a relaxation scheme, a restriction operator which interpolates a function from the fine grid to the coarse grid, a coarse-grid operator, and a prolongation operator interpolating a function from the coarse grid to the fine grid. The fine grid problem for the present example may be written

$$L^f U^f = F^f \ . \tag{81}$$

Let V^f denote the fine-grid approximation. After the high-frequency content of the error $V^f - U^f$ has been sufficiently damped, attention shifts to the coarse grid. The coarse-grid problem is

$$L^c U^c = F^c \tag{82}$$

where

$$F^c = R\,[F^f - L^f\,V^f]\ ,$$

R being the restriction operator. After a satisfactory approxmation, V^c is obtained; the coarse-grid correction $(V^c - RV^f)$ is interpolated onto the fine grid by the prolongation operator P, yielding the corrected fine-grid solution

$$V^f \leftarrow V^f + P\,(V^c - RV^f) \tag{83}$$

The details of spectral multigrid techniques are furnished in [40]. Spectral multigrid techniques have been used to solve a variety of problems including the transonic full potential equation [41, 42]. Additional applications of spectral methods to compressible flows are described in [42].

2.1.3 Convection-Dominated Flows

A model for convection-dominated flows is the viscous Burger's equation,

$$u_t + (u^2)_x/2 = \nu u_{xx} \qquad u(x,t=0) = -\sin\pi x, \tag{84}$$

with boundary conditions $u(-1) = u(1) = 0$, and "small diffusivity," $\nu = .01/\pi$ [43]. The solution to this problem develops a near shock. This near shock is characterized by the time at which the derivative at the origin attains a maximum value, t_{max}, and the value of its maximum derivative, $|\partial u/\partial x|_{max}$. The convective term is clearly dominant for short times, however the diffusion term insures that the solution will be smooth. This convection-diffusion balance is a good model for the kind of phenomena that arise in solution of the incompressible Navier-Stokes equations. The critical numer-

ical issues are numerical dispersion and diffusion. The former leads to incorrect propagation speeds of the shock affecting t_{max}. The latter leads to smearing of the shock affecting $|\partial u/\partial x|_{max}$.

This problem has been solved by a variety of methods, including the spectral element method [43] and the explicit flux balancing method [37]. The spectral element calculations have used Crank-Nicolson in time on the diffusion term and the resulting Helmholtz equation in space was solved using the variational methods presented in Section 2.1.1. The convective term was handled by explicit third-order Adams-Bashforth. Four elements were used covering the intervals [-1., -0.05], [-0.05, 0], [0., 0.05], [0.05, 1.] which cluster points around the location of high function variation. Macaraeg and Streett [37] used three subdomains with their flux conservation method. Table III presents a comparison of various methods on this model problem.

2.2. INCOMPRESSIBLE NAVIER-STOKES EQUATIONS

This section is devoted to a description of algorithms for the solution of the incompressible Navier-Stokes equations in primitive variable form. The algorithms are based on methods discussed in the previous section in the simplest context. For example, simulation of instability and transition to turbulence in a flat-plate boundary layer have used iterative methods described in section 2.1.2. The spectral element method has been used for a variety of flow computations, including the problem of flow past a cylinder.

The Navier-Stokes equations in the so-called rotation form are

$$q_t = q \times \omega + \nabla \cdot (\mu \nabla q) - \nabla P \qquad \text{in } D$$

$$\nabla \cdot q = 0 \qquad \text{in } D \tag{85}$$

$$q(x,0) = q_0(x) \qquad \text{in } D$$

and

$$q = g \qquad \text{on } \partial D$$

where $q = (u,v,w)$ is the velocity vector, $\omega = \nabla \times q$ the vorticity, $P = p + 1/2\ |q|^2$ the total pressure, μ the variable viscosity, D the interior of the domain, and ∂D its boundary. In the stability and transition problems, the domain D is cartesian and semi-infinite: periodic in the two horizontal directions (x,z), and bounded by a wall at $y=0$. Fourier collocation can be used in the periodic directions (x,z) and Chebyshev collocation is used in the vertical (y) direction. The collocation points in the periodic directions are given by a relation similar to Eq. (11). The vertical extent of the domain $0 < y < \infty$ is mapped onto $-1 < \xi < +1$. The velocities are defined and the momentum equations enforced at the points

$$\xi_j = \cos\left(\frac{\pi j}{N_y}\right), \qquad j = 0,\ 1,\ \ldots,\ N_y \tag{86}$$

The pressure is defined at the half points

$$\xi_{j+\frac{1}{2}} = \cos\left[\frac{\pi\ (j+1/2)}{N_y}\right], \qquad j = 0,\ 1,\ \ldots,\ N_y - 1 \tag{87}$$

and the continuity equation is enforced at these points. The staggered grid avoids artificial pressure boundary conditions, and precludes spurious pressure modes.

After a Fourier transform in x and z, the temporal discretization (backward Euler for pressure, Crank-Nicolson for normal diffusion, and third or fourth-order Runge-Kutta for the remaining terms) of Eq. (85) leads to

$$[I - MDM]\, Q + \Delta t\, A_0\, \nabla \Pi = Q_c \tag{88}$$

$$-A_+ \nabla \cdot Q = 0$$

where

$$Q = \{\tilde{q}_0^{n+1}, \tilde{q}_1^{n+1}, \ldots, \tilde{q}_N^{n+1}\}$$

$$\Pi = \{\tilde{p}_{1/2}^{n+1}, \hat{p}_{3/2}^{n+1}, \ldots, \hat{p}_{N-1/2}^{n+1}\} \tag{89}$$

$$\nabla = \{ik_x \frac{\partial}{\partial y}, ik_x\}$$

M is the Chebyshev derivative operator, D the diagonal matrix with $1/2\mu\Delta t$ as its elements, and A_0 is the interpolation operator from the half points to cell faces, A_+ vice versa. Obviously, the equations for each pair of horizontal wave number (k_x, k_x) are indepenent and they can be written as the system

$$LX = F \tag{90}$$

where $X = [Q, \Pi]$. The iterative solution of this equation is carried out by preconditioning the system with a finite difference approximation on the Chebyshev grid, and applying a standard iterative technique such as Richardson, minimum residual or multigrid [44].

The method described above solves the implicit equations together as a set. The extension of this method to the more general cases of interest such as those involving two or more inhomogeneous directions is not straightforward. An alternative is the operator-splitting technique or the fractional step scheme [45]. This method yields implicit matrices which are positive definite and are easily amenable to iterative methods. In the first step, one solves the advection-diffusion equation

$$q_t^* = q^* \times \omega^* + \nabla \cdot (\mu \nabla q^*) \tag{91}$$

subject to the initial and boundary conditions

$$\begin{aligned} q^*(x,t_n) &= q(x,t_n). \\ q^* &= g^* \quad \text{on } \partial D. \end{aligned} \tag{92}$$

Note that g^* has yet to be defined. In the second step, one solves for the pressure correction

$$q_t^{**} = -\nabla P^{**} \tag{93}$$

$$\nabla \cdot q^{**} = 0 \tag{94}$$

subject to the conditions

$$\begin{aligned} q^{**}(x,t^*) &= q^*(x,t^*) && \text{in } D \\ g^{**} \cdot \hat{n} &= g \cdot \hat{n} && \text{in } \partial\Omega \end{aligned} \tag{95}$$

where $\hat{n}$ is the unit normal to the boundary. Further, the tangential

component of the Eq. (95) holds on the boundary, i.e.,

$$q_t^{**} \cdot \hat{\tau} = - \nabla P^{**} \cdot \hat{\tau} \qquad \text{in } \partial D \tag{96}$$

where $\hat{\tau}$ is a unit tangent vector to the boundary. Now g^* is defined [45] as (using Taylor expansion in t)

$$g^* \cdot \hat{n} = (g^n + \Delta t \; g_t^n) \cdot \hat{n} \tag{97}$$

$$g^* \cdot \hat{\tau} = [g^n + \Delta t \; (g_t^n + \nabla P^n)] \cdot \hat{\tau} \; .$$

Eq. (91) is discretized in the usual spectral collocation manner. After a temporal and spatial discretization of Eq. (93), the boundary conditions are built into the relevant matrix operators, and then a discrete divergence is taken. This results in a discrete Poisson equation (with as many algebraic equations as unknowns) for pressure, which can be solved by standard iterative techniques including the multigrid method.

Spectral element methods have been applied to the incompressible Navier-Stokes equations (85). In addition to (98), the uncoupled (passive) or coupled (natural convection) energy equation is also often of interest. The time discretization used for the Navier-Stokes equations is either a Green's function technique [29] or an operator splitting scheme [30]. Both of these methods reduce (85) at each time step to an initial convective step, followed by a Stokes problem consisting of a sequence of Poisson and Helmholtz equations. The spatial discretizations discussed above in Section 2.1.1 are directly applicable to these Navier-Stokes subproblems.

Spectral element methods have been applied to the simulation of numerous flows in the Reynolds number range $0 < R < 1500$ [36, 46 - 47]. An example is provided by the classical problem of flow past a cylinder. Results are presented here for $R = 100$, based on freestream velocity and cylinder diameter, for times sufficiently large that the flow has reached a steady-periodic state. Figure 6 shows the spectral element mesh used, and Figures 7 and 8 show the streamlines and isotherms, respectively, at one time in the periodic flow cycle. The thermal boundary conditions are $T = T_\infty$ far from the cylinder, and $T = T_w$ on the cylinder surface. The isotherm pattern clearly reveals the spatial structure of the von Karman vortex street. Note the minimal numerical dispersion in the scheme, as evidenced by the clear identity of the shed packets of fluid and the absence of trailing waves in the wake. More details of these cylinder calculations, as well as comparisons with previous numerical work and experiment, can be found in [36].

2.3 HYPERBOLIC EQUATIONS

Here, the application of spectral methods to the solution of inviscid compressible flow problems is surveyed. Methods for such problems are not nearly so advanced as those for incompressible flows. The survey is limited to methods for the solution of the Euler equations of gas-dynamics governing some flows of aerodynamic interest. For the solution of the full potential equation for transonic flows, see Streett, et al. [42].

The Euler equations of gas-dynamics are a coupled system of nonlinear hyperbolic equations which (in one dimension) are usually written in the conservative form

$$u_t + F_x(u) = H. \tag{98}$$

Typically, spectral discretization in space and explicit finite difference discretization in time are used. The discontinuous solutions of this set of equations have been obtained in the case of a shock tube (Gottlieb, Lustman, and Orszag [48], Cornille [49]), quasi-one-dimensional flow in a nozzle (Zang and Hussaini [50]) and for the astrophysical problem of shocked flow in a galaxy (Hussaini, et al. [51]).

The astrophysical problem is the most challenging one-dimensional compressible flow problem for which shock capturing has been attempted with a Fourier spectral method. It contains a strong shock and an adjacent strong expansion. Unlike problems with weak shocks and expansions, it was necessary to apply strong filtering to stabilize the numerical solution. The result of this drastic filtering was a reduction of the order of accuracy. Even in the smooth parts of the solution away from the shock, the accuracy was only first order. In view of the extra work involved to compute the spectral approximations, it is not clear that spectral methods with filtering are a viable alternative to finite difference methods when strong shocks are captured.

An alternative to capturing shocks is to treat them as boundaries. In this case, it is possible to compute the solutions using the nonconservative form

$$Q_t + AQ_x = E \tag{99}$$

along with an ordinary differential equation for the motion of the shock. A number of two dimensional shock-fitted solutions are described in Hussaini, et al. [52]. These solutions include a shock/turbulence interaction.

Shock/vortex interaction and supersonic flow past a cylinder. When shocks are fitted, spectral methods do indeed outperform typical second order finite difference methods, as long as the solution is adequately resolved. Kopriva, et al. [53] compared the performance between MacCormack's method and the spectral collocation method for the shock/plane wave interaction problem and for the Ringleb problem. A comparison of the accuracy of the finite difference method vs. the spectral method is shown in Table IV.

A multidomain method for the nonconservative form of the Euler equations suitable for use with shock-fitting has been described by Kopriva [54]. In each subdomain, the usual collocation method (Section 1.2.2) is applied. At interfaces, however, a weighted average of the derivatives is used. In one dimension,

$$Q_t^I + A^L Q_x^L + A^R Q_x^R = E \tag{100}$$

where Q^I denotes the solution vector at the interface and the derivatives superscripted with the L and R denote the left and right computed spectral approximations. For consistency, $A^L + A^R = A$. The weighting corresponds to an upwind approximation

$$A^L = 1/2(A + |A|) \qquad A^R = 1/2(A - |A|)$$

where $|A| = Z|\Lambda|Z^{-1}$ and Z is the matrix of right eigenvectors. For many applications, this can be simplified by replacing $|A|$ by a diagonal approximation $|A| \approx \lambda^* I$ where $|\lambda|_{min} < \lambda^* < |\lambda|_{max}$ is an approximation to the eigenvalues of A.

Subdividing the domain retains spectral accuracy. Table V shows the performance of a two domain computation of a one dimensional 2×2 hyperbolic system

$$\begin{bmatrix} u \\ v \end{bmatrix}_t + \begin{bmatrix} 1 & 2 \\ 2 & 1 \end{bmatrix} \begin{bmatrix} u \\ v \end{bmatrix}_x = 0 \tag{102}$$

from [54] with solution u and v for an equal number of points on each side of the interface.

For a given number of grid points, it is possible to obtain solutions with a multidomain spectral method which are significantly better than the single domain method. For the two dimensional nonlinear Ringleb problem computed by Kopriva [54], Table VI shows the effect on the error of a four domain division in which the position of the streamwise interface is varied. The accuracy is best when rapid changes in the solution are best resolved.

The shock-vortex interaction problem described by Kopriva [55] provides another example of the advantage of a multidomain method over a single domain method. A two dimensional region between the shock and an arbitrary upstream boundary is mapped onto a square. The shock moves downstream where it encounters a vortex. The interaction of the shock and the vortex creates a circular sound wave centered on the vortex. Because the physical domain is continually increasing in size, the resolution of the solution decreases with time.

The single domain solution to the shock-vortex problem cannot be computed without added smoothing. Figure 9a shows the pressure contours with no smoothing. The numerical oscillations in the pressure are of the same order as the sound pressure wave created by the interaction. If the region between

the shock and the upstream boundary is subdivided and some of the subdomains are allowed to move with the shock, smoothing is not required. Figure 9b shows the pressure contours of a two domain calculation with the same number of grid points in the horizontal direction. The horizontal numerical oscillations are no longer present and the sound pressure wave is clearly visible.

REFERENCES

1. Gottlieb D. and S. A. Orszag, "Numerical analysis of spectral methods: Theory and application," SIAM-CBMS, Philadelphia, 1977.

2. Quarteroni, A., "Theoretical motivations underlying spectral methods", Proc. Meeting I.N.R.I.A.-Novosibirsk, Paris, December 1983.

3. Courant, R. and D. Hilbert, Methods of Mathematical Physics, Vol. I, Interscience, New York, 1953.

4. Hussaini, M. Y., C. Streett, and T. A. Zang, "Spectral methods for partial differential equations," ARO Report 84-1, pp. 883-925.

5. Davis, P. J. and P. Rabbinowitz, Methods of Numerical Integration, 2nd Edition, Academic Press, New York, 1984.

6. Gottlieb, D. , M. Y. Hussaini, and S. Orszag, "Theory and application of spectral methods" in Spectral Methods for Partial Differential Equations, SIAM, Philadelphia, 1984.

7. Kreiss, H.-O. and J. Oliger, "Approximate solution of time dependent problems," GARP Rept. #10, World Meteorological Organization, 1973.

8. Pasciak, J. E. "Spectral and pseudospectral methods for advection equations," Math. Comp., Vol. 35, 1980, pp. 1081-1092.

9. Canuto, C. and A. Quarteroni, "Approximation results for orthogonal polynomials in Sobolev spaces," Math. Comp., Vol. 38, 1982, pp. 67-86.

10. Mercier, B., "Analyse numerique des methodes spectrales," Note CEA-N-2278, Commisariat A L´Energie Atomique, June 1981.

11. Tadmor, E. "The exponential accuracy of Fourier and Tchebyshev differencing methods," SIAM J. Numer. Anal., Vol. 23, 1986, pp. 1-10.

12. Majda, A., J. McDonough, and S. Osher, "The Fourier method for nonsmooth initial data," Math. Comp., Vol. 32, 1978, pp. 1041-1081.

13. Gottlieb, D. and E. Tadmor, "Recovering pointwise values of discontinuous data within spectral accuracy," ICASE Report No. 85-3, 1985.

14. Canuto, C. and A. Quarteroni, "Variational methods in the theoretical analysis of spectral methods," in Spectral Methods for Partial Differential Equations, SIAM, Philadelphia, 1984, pp. 55-78.

15. Canuto, C., "Recent advances in the analysis of Chebyshev and Legendre spectral methods for boundary value problems," in Glowinski and Lions (Editors) Computing Methods in Applied Science and Engineering, VI North Holland (Amsterdam, New York), 1984.

16. Canuto, C., "Boundary conditions in Chebyshev and Legendre methods," SIAM J. Numer. Anal., Vol. 23, 1986, pp. 815-831.

17. Kreiss, H.-O. and J. Oliger, "Stability of the Fourier method" SIAM J. Numer. Anal., Vol. 16, 1979, pp. 421-433.

18. Gottlieb, D., "The stability of pseudospectral-Chebyshev methods," Math. Comp., Vol. 36, 1981, pp. 107-118.

19. Canuto, C. and A. Quarteroni, "Spectral and pseudospectral methods for parabolic problems with non-periodic boundary conditions," Calcolo, Vol. 23, 1981, pp. 197-217.

20. Kreiss, H.-O. and J. Oliger, "Comparison of accurate methods for the integration of hyperbolic equations," Tellus, Vol. 24, 1972, pp. 199-215.

21. Tadmor, E., "Skew-selfadjoint form for systems of conservation laws," J. Math. Anal. Appl., Vol. 103, 1984, pp. 428-442.

22. Gottlieb, D., S. A. Orszag, and E. Turkel, "Stability of pseudospectral and finite-difference methods for variable coefficient problems," Math. Comp., Vol. 37, 1981, pp. 293-305.

23. Canuto, C. and A. Quarteroni, "Error estimates for spectral and pseudo-spectral approximations of hyperbolic equations," SIAM J. Numer. Anal., Vol. 19, 1982, pp. 629-642.

24. Reyna, L. G. M., "Stability of Chebyshev collocation," Ph.D. Thesis, California Institute of Technology, 1982.

25. Gottlieb, D., L. Lustman, and E. Tadmor, "Stability analysis of spectral methods for hyperbolic initial-boundary value systems," ICASE Report No. 86-2, NASA CR-178041, 1986.

26. Gottlieb, D., L. Lustman, and E. Tadmor, "Convergence of spectral methods for hyperbolic initial-boundary value systems," ICASE Report No. 86-8, NASA CR-178063, 1986.

27. Orszag, S. A., "Spectral methods for problems in complex geometries," J. Comp. Phys., Vol. 37, 1980, p. 70.

28. Morchoisne, "Inhomogeneous flow calculations by spectral methods: Mono-domain and multidomain techniques," in Spectral Methods for Partial Differential Equations, D. Gottlieb, M. Y. Hussaini, and R. G. Voigt (Editors), SIAM Philadelphia, 1984, p. 181.

29. Patera, A. T., "A spectral element method for fluid dynamics; laminar flow in a channel expansion," J. Comput. Phys., Vol. 54, 1984, pp. 468-488.

30. Korczak, K. Z. and A. T. Patera, "An isoparametric spectral element method for solution of the Navier-Stokes equations in complex geometry," J. Comput. Phys., Vol. 62, 1986, pp. 361-382.

31. Strang, G. and G. J. Fix, "An analysis of the finite element method," Prentice-Hall, New Jersey, 1973.

32. Babuska, I. and M. R. Dorr, "Error estimates for the combined h and p versions of the finite element method," Numer. Math., Vol. 37, 1980, p. 267.

33. Delves, L. M. and C. A. Hall, " An implicit matching procedure for global element calculations," J. Inst. Math. Appl., Vol. 23, 1979, p. 223.

34. Bullister, E. T., G. E. Karniadakis, E. M. Ronquist, and A. T. Patera, "Solution of the unsteady Navier-Stokes equations by spectral element methods," in Proc. Sixth Int. Symp. on Finite Element Methods in Flow Problems, Antibes, 1986.

35. Patera, A. T., "Fast direct Poisson solvers for high-order finite element discretizations in rectangularly-decomposable domains," J. Comput. Phys., Vol. 65, 1986, pp. 474-480.

36. Karniadakis, G. E., E. T. Bullister, and A. T. Patera, "A spectral element method for the two- and three-dimensional time-dependent incompressible Navier-Stokes equations," in Proc. Europe-U.S. Symp. on Finite Element Methods for Nonlinear Problems, Norway, Springer, 1986.

37. Macaraeg, M. G. and C. L. Streett, "Improvements in spectral collocation through a multiple domain technique," Appl. Numer. Math., Vol. 2., 1986, pp. 95-108.

38. Macaraeg, M. G. and C. L. Streett, "A spectral multi-domain technique with application to generalized curvilinear coordinates," NASA TM 87701, 1986.

39. Gottlieb, D. and S. A. Orszag, "Numerical analysis of spectral methods: Theory and applications," CBMS-NSF Regional Conference Series in Applied Mathematics, SIAM, 1977.

40. Zang, T. A., Y-S. Wong, and M. Y. Hussaini, "Spectral multigrid methods for elliptic equations," J. Comput. Phys., 1982, Vol. 48, pp. 485-501 and Vol. 54, pp. 489-507.

41. Streett, C. L., T. A. Zang, and M. Y. Hussaini, "Spectral multigrid methods with applications to transonic potential flow," J. Comput. Phys., Vol. 57, 1985, pp. 43, 76.

42. Hussaini, M. Y., M. D. Salas, and T. A. Zang, "Spectral methods for inviscid, compressible flows," Advances in Computational Transonics, pp. 875-912, W. G. Habashi (ed.), Pineridge Press, Swansea, 1985.

43. Basdevant, C., M. Deville, P. Haldenwang, J. M. Lacroix, J. Ouazzani, R. Peyret, P. Orlandi, and A. T. Patera, "Spectral and finite difference solutions of the Burgers equation," Computers and Fluids, Vol. 14, 1986, pp. 23-41.

44. Zang, T. A. and M. Y. Hussaini, "Numerical experiments on subcritical transition mechanisms," AIAA Paper No. 85-0296, 1985.

45. Zang, T. A. and M. Y. Hussaini, "On spectral multigrid methods for time-dependent Navier-Stokes equations," Appl. Math. Comp., Vol. 19, 1986, pp. 359-372.

46. Ghaddar, N. K., K. Z. Korczak, B. B. Mikic, and A. T. Patera, "Numerical investigation of incompressible flow in grooved channels. Part 1: Stability and self-sustained oscillations," J. Fluid Mech., Vol. 163, 1986, pp. 99-127.

47. Ghaddar, N. K., M. Magen, B. B. Mikic, and A. T. Patera, "Numerical investigation of incompressible flow in grooved channels. Part 2: Resonance and oscillatory heat transfer enhancement," J. Fluid Mech., Vol. 168, 1986, pp. 541-567.

48. Gottlieb, D., L. Lustman, and S. A. Orszag, "Spectral calculations of one dimensional inviscid compressible flows," SIAM J. Sci. Stat. Comp., Vol. 2, 1981, pp. 296-310.

49. Cornille, P., "A pseudospectral scheme for the numerical calculation of shocks," J. Comp. Phys., Vol. 47, 1982, pp. 146-159.

50. Zang, T. Z. and M. Y. Hussaini, "Mixed spectral-finite difference approximations for slightly viscous flows," Proceedings of the 7th International Conference on Numerical Methods in Fluid Dynamics, W. C. Reynolds and R. W. MacCormack (Editors), Lecture Notes in Physics, No. 141, Springer-Verlag, New York, 1981, pp. 461-446.

51. Hussaini, M. Y., D. A. Kopriva, M. D. Salas, and T. A. Zang, "Spectral methods for the Euler equations. Part 1: Fourier methods and shock-capturing," AIAA J., Vol. 23, 1985, pp. 64-70.

52. Hussaini, M. Y., D. A. Kopriva, M. D. Salas, and T. A. Zang, "Spectral methods for the Euler equations: Part II - Chebyshev methods and shock fitting," AIAA J., Vol. 23, 1985, pp. 234-340.

53. Kopriva, D. A., T. A. Zang, M. D. Salas, and M. Y. Hussaini, "Pseudo-spectral solution of two dimensional gas dynamics problems," Proc. 5th GAMM Conference on Numerical Methods on Fluid Mechanics, M. Pandolfi and R. Piva (Editors), Friedr Vieweg & Sohn, Braunschweig, Wiesbaden, 1983, pp. 185-192.

54. Kopriva, D. A., "A spectral multidomain method for the solution of hyperbolic systems," Applied Numerical Mathematics, Vol. 2, 1986, pp. 221-241.

55. Kopriva, D. A., "A multidomain spectral collocation computation of the sound generated by a shock-vortex interaction," Proc. First IMACS Symposium on Computational Acoustics, Yale University, 1986.

FIGURE CAPTIONS

Figure 1. The domain and Legendre spectral element discretization used for solution of the Laplace equation described in the text. Although results are given for a single isoparametric element, similar results are obtained with multiple elements. (Legendre results due to E. M. Ronquist.)

Figure 2. A plot of the L_∞ error as a function of the number of points in one direction for solution of Laplace's equation in the domain shown in Figure 1.

Figure 3. Description of the domain and boundaries for the Stefan problem presented in the text. (Stefan problem results due to E. M. Ronquist.)

Figure 4. Spectral element prediction for the position of the interface, ∂D_I, for the Stefan problem described in the text. The spectral element mesh uses two elements, one each in each phase.

Figure 5. Temperature (θ) distribution for the Stefan problem described in the text. Note the discontinuity of slope at the interface, ∂D_I.

Figure 6. Spectral element mesh used for simulation of flow past a cylinder. Note the flexible resolution afforded by the elemental decomposition. (Flow past a cylinder results due to G. E. Karniadakis.)

Figure 7. Instantaneous streamlines of the cylinder flow at a Reynolds number of $R = 100$.

Figure 8. Instantaneous isotherms of the cylinder flow at a Reynolds number of $R = 100$ (Prandtl number of unity). The von Karman vortex street can be clearly seen in the temperature distribution behind the cylinder.

Figure 9. Pressure contours for a shock/vortex interaction. (a) Single domain calculation. (b) Three vertical domain calculation.

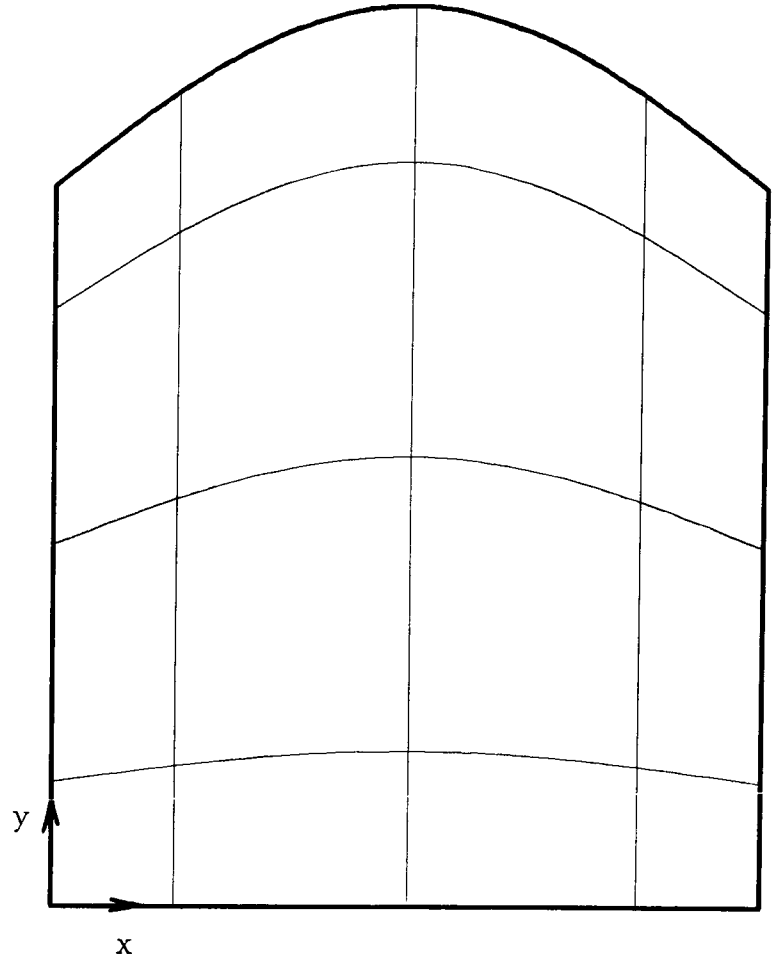

Figure 1.

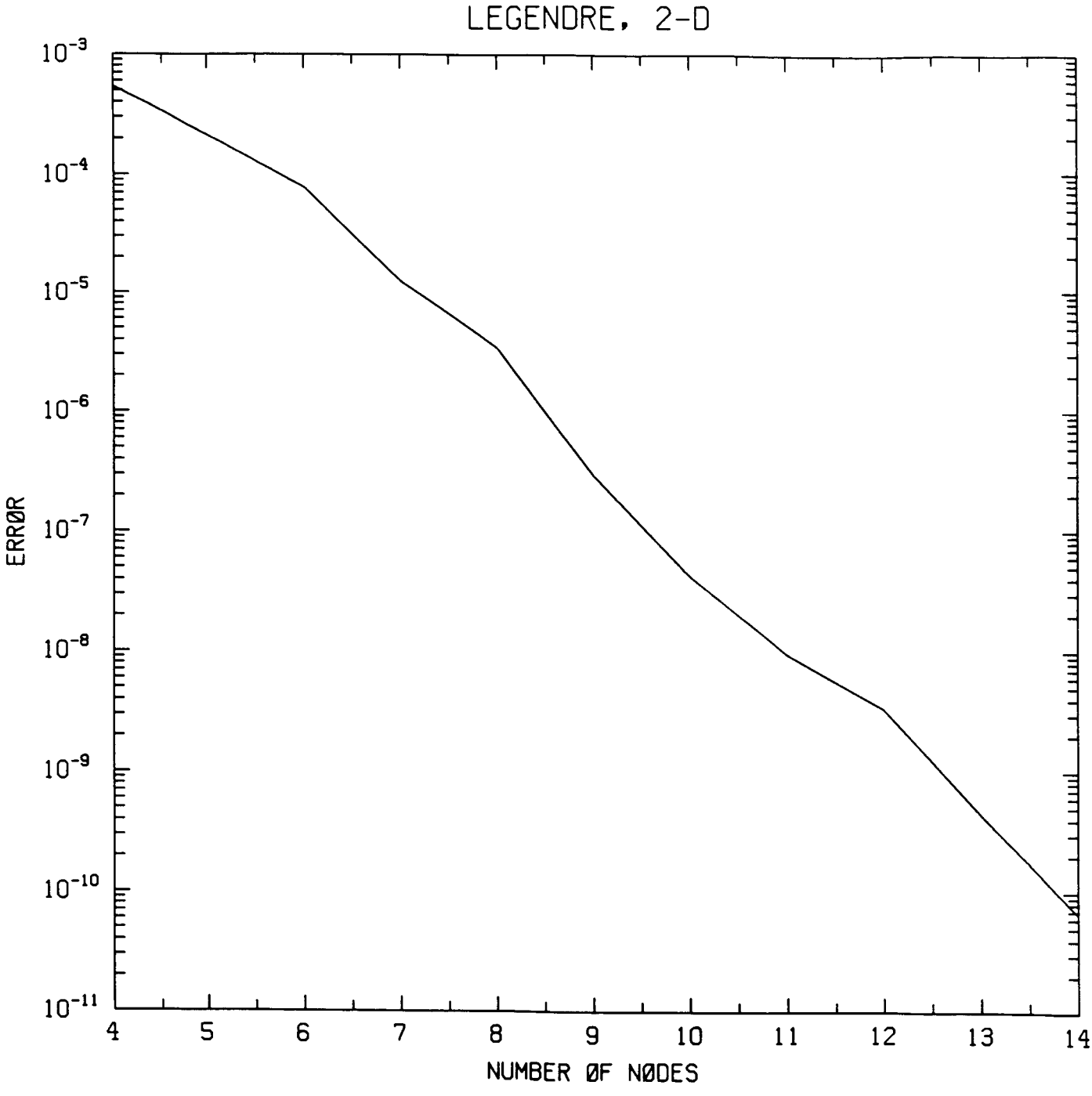
LEGENDRE, 2-D
ERRØR
10^{-3}
10^{-4}
10^{-5}
10^{-6}
10^{-7}
10^{-8}
10^{-9}
10^{-10}
10^{-11}
4
5
6
7
8
9
10
11
12
13
14
NUMBER ØF NØDES

Figure 2.

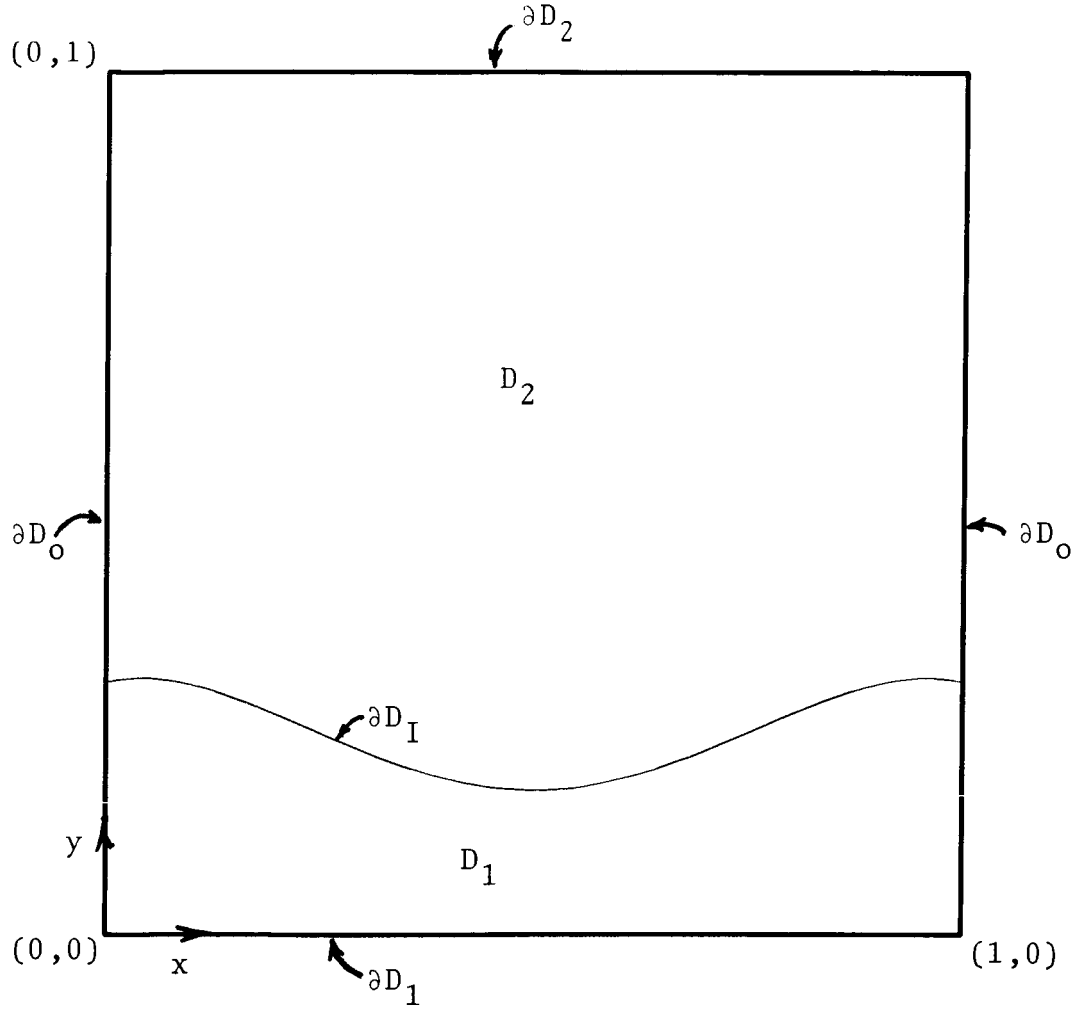

Figure 3.

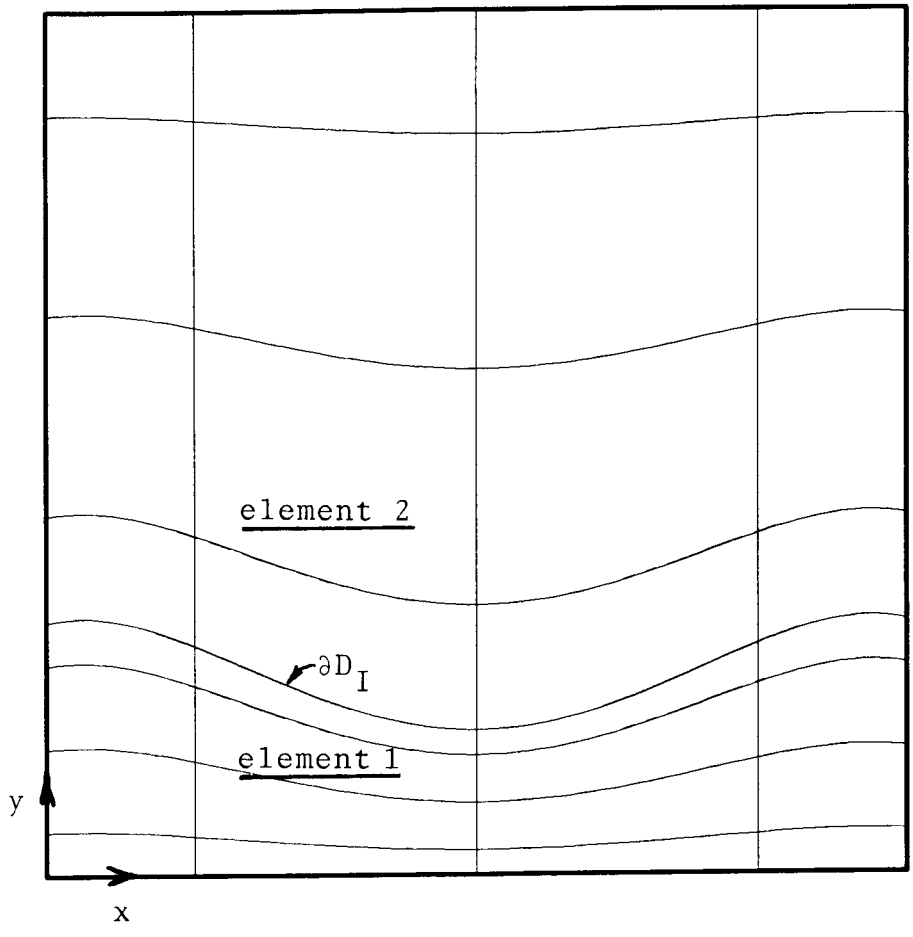

Figure 4.

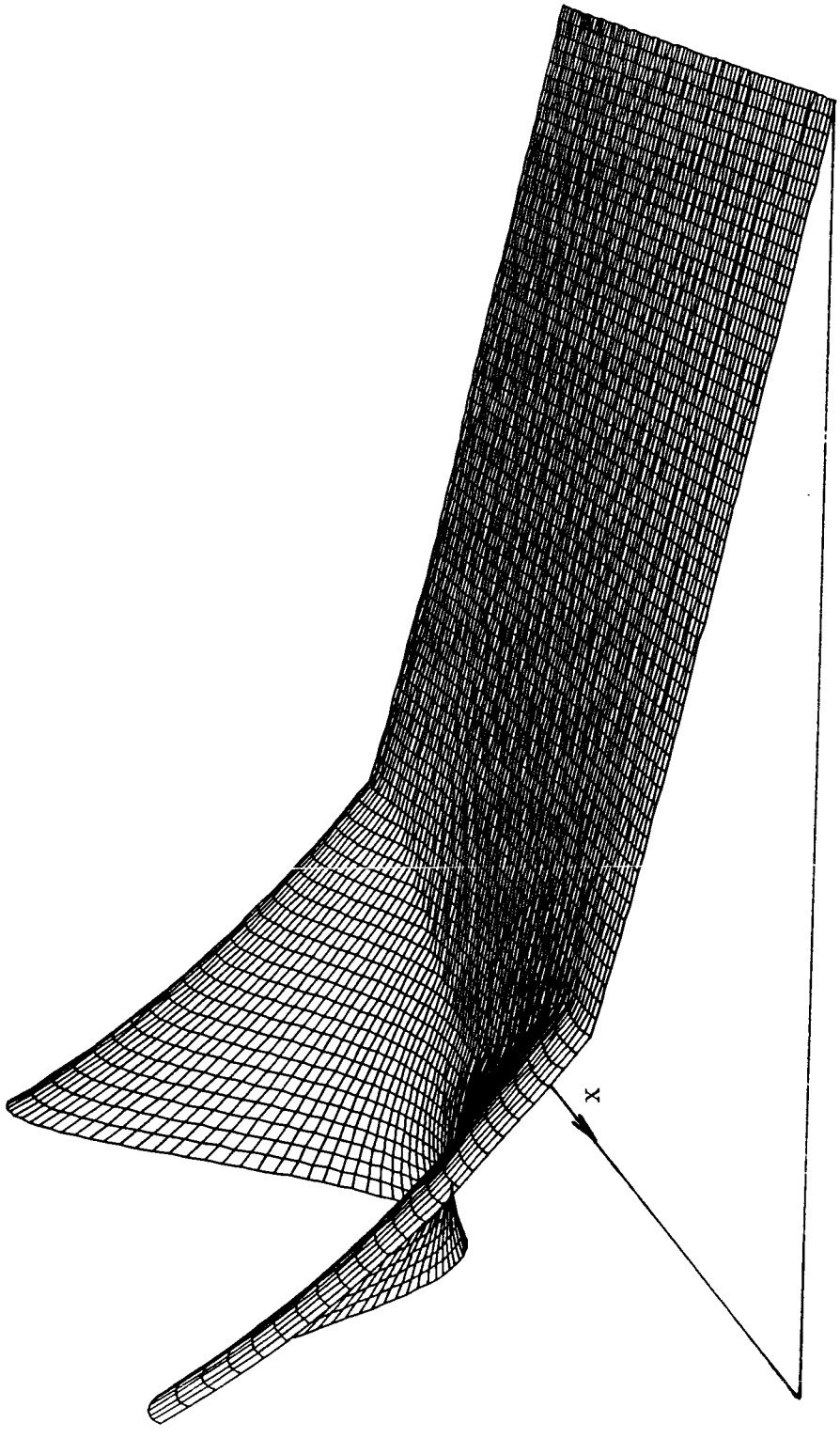

Figure 5.

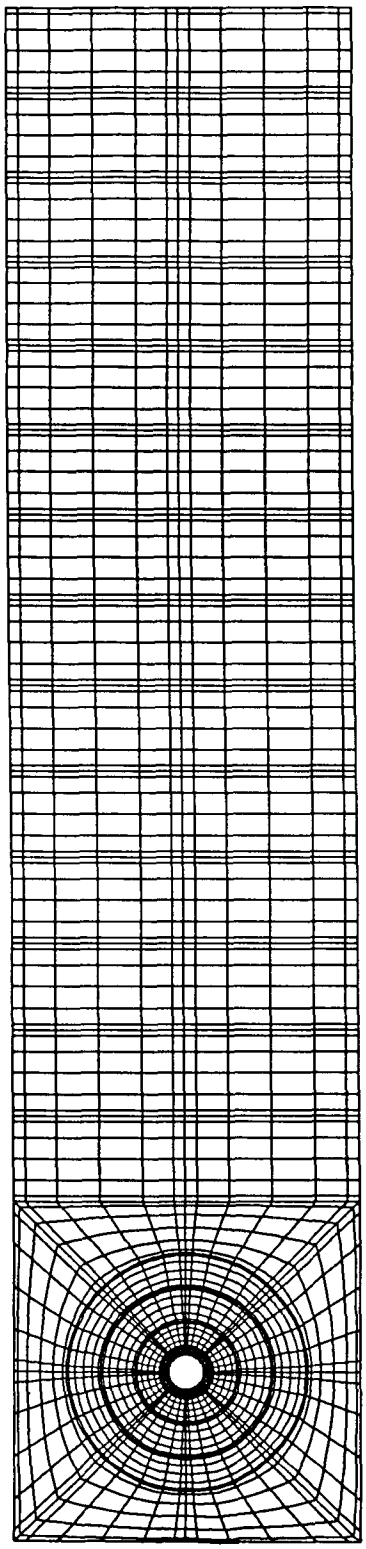

Figure 6.

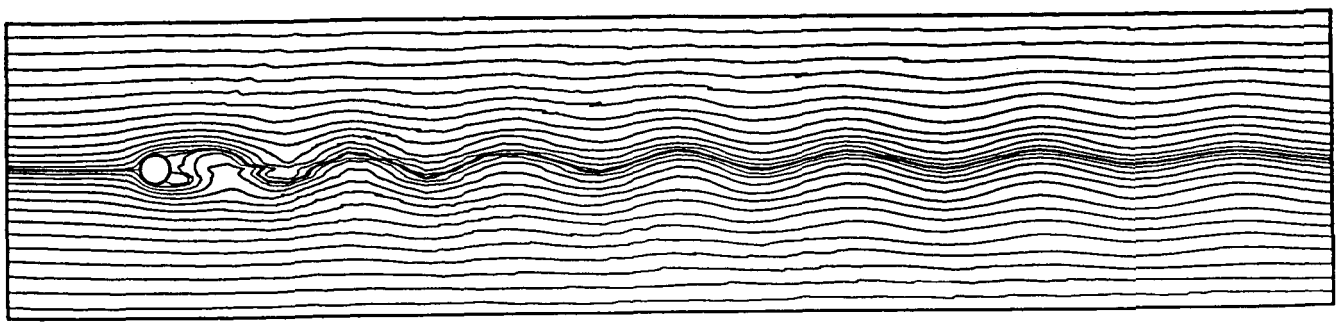

Figure 7.

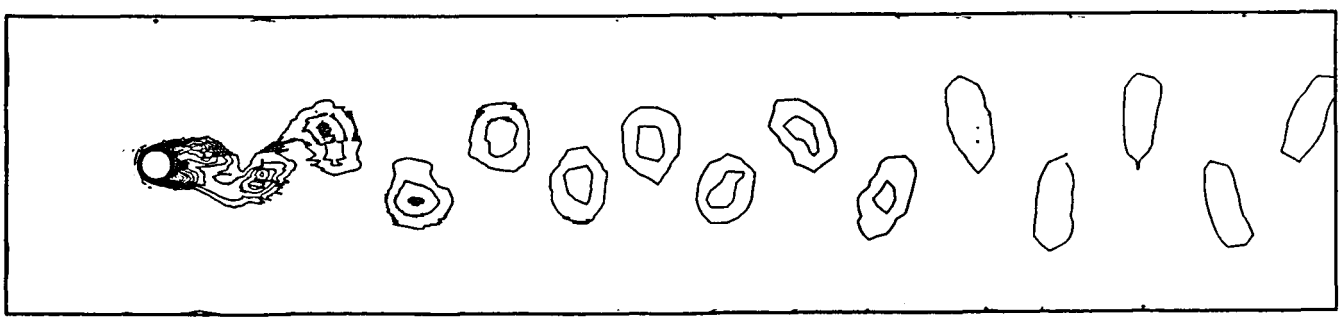

Figure 8.

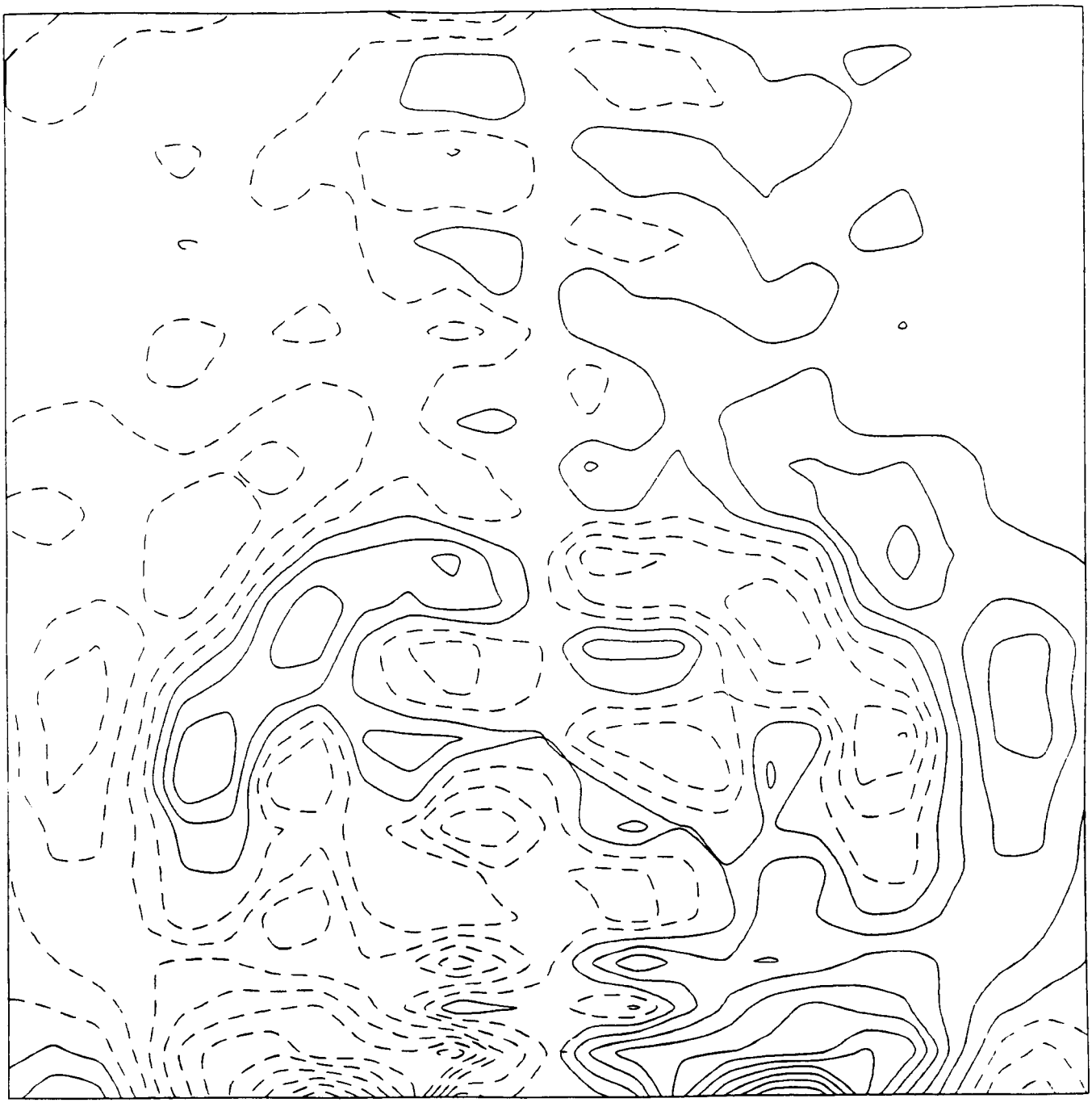

Figure 9a.

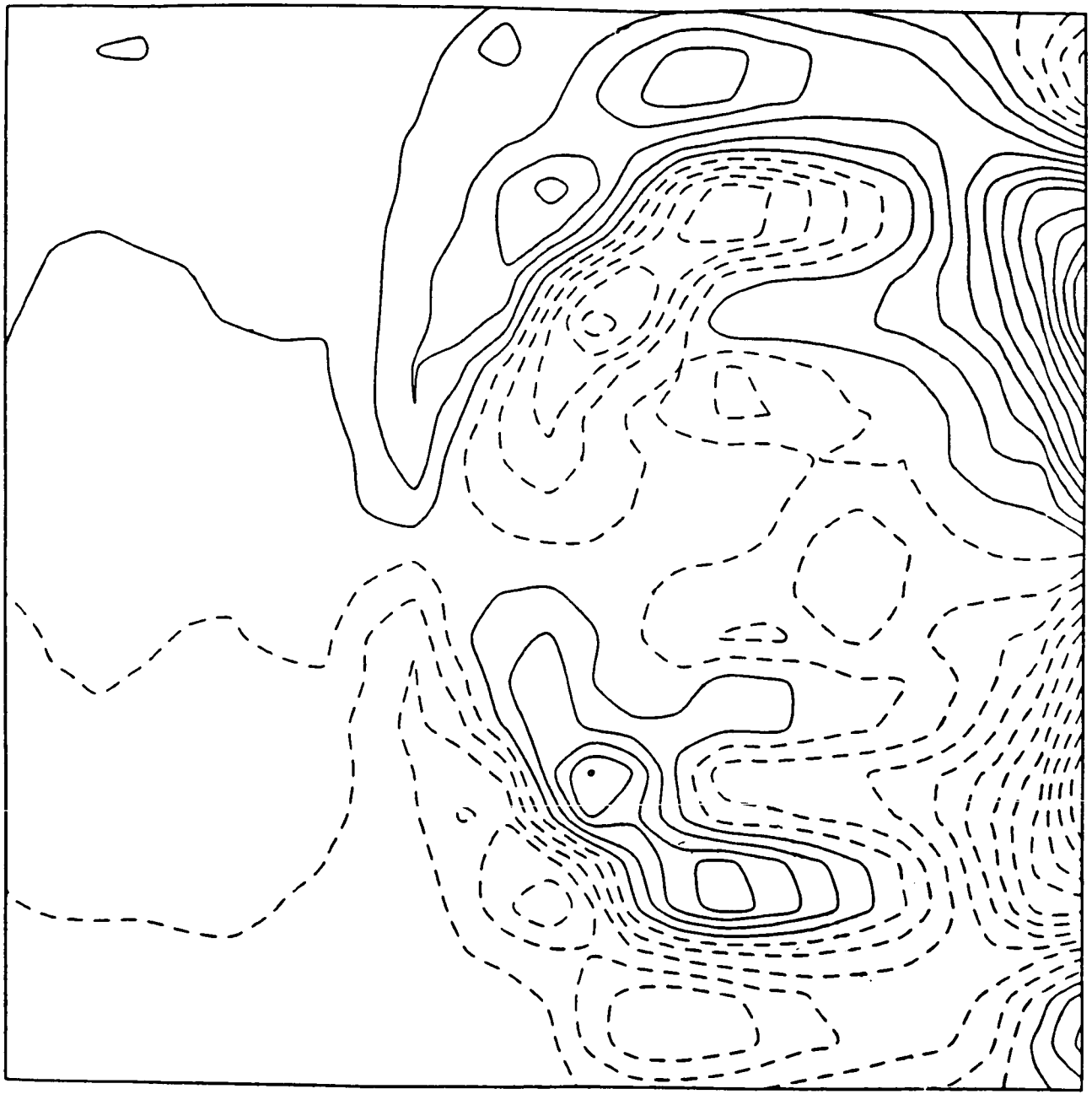

Figure 9b.

Table 1. Preconditioned Eigenvalues for One-dimensional First Derivative Model Problem

Preconditioning	Eigenvalues
Central Differences	$\frac{k\Delta x}{\sin(k\Delta x)}$
High Mode Cutoff	$\frac{k\Delta x}{\sin(k\Delta x)}$ $\quad \lvert k\Delta x\rvert \leq (2\pi/3)$
	$0 \quad (2\pi/3) < \lvert k\Delta x\rvert \leq \pi$
One-sided Differences	$e^{-i(k\Delta x/2)} \frac{k\Delta x/2}{\sin((k\Delta x)/2)}$
Staggered Grid	$\frac{(k\Delta x)/2}{\sin((k\Delta x)/2}$

Table 2. Damping Factors for N = 64

p	Single-Grid	Multigrid
1	.9980	.9984
2	.9922	.9938
4	.9688	.9750
8	.8751	.9000
12	.7190	.7750
16	.5005	.6000
20	.2195	.3750
24	.1239	.1000
28	.5298	.2250
32	.9980	.6000

Table III. Comparison of Methods for Solution of Burger's Equation (from Ref. 43, 37)

Method	Interval	$\left\|\frac{\partial u}{\partial x}\right\|_{max}$	$\pi \cdot t_{max}$	N/M	$\Delta t \cdot \pi$
- Fourier Galerkin	[-1,1]	151.942	1.6035	682/1024	5.10^{-4}
		142.665	1.60	682/1024	10^{-2}
		148.975	1.603	170/256	5.10^{-4}
		142.313	1.60	170/256	10^{-2}
- Fourier Pseudospectral	[-1,1]	142.606	1.60	256/256	10^{-2}
		144.237	1.60	128/128	10^{-2}
- ABCN collocation	[-1,1]	145.877	1.60	512	5.10^{-3}
+coordinate transform	[-1,1]	152.123	1.60	64	10^{-2}
- Spectral Element	[-1,1]	152.04	1.6033	16 x 4	$10^{-2}/6$
- FD	[-1,1]	150.1	1.63	81	10^{-2}
- Chebyshev					
ABCN spectral	[0,1]	152.05	1.60	64	1/300
Rosenbrook spectral	[0,1]	151.998	1.60	64	10^{-2}
	[0,1]	150.144	1.60	32	10^{-2}
ABCN collocation	[0,1]	152.126	1.60	64	10^{-2}
- Flux balance	[-1,1]	152.00011			
- Analytical		152.00516	1.6037		

Table IV. Maximum Error in p for MacCormack and Spectral Computation of Transonic Ringleb Flow

Grid	MacCormack	Spectral
9 x 5	2.6×10^{-2}	2.2×10^{-2}
17 x 9	1.1×10^{-2}	1.9×10^{-3}
33 x 17	3.2×10^{-3}	5.0×10^{-5}

Table V. Solutions to (102) with Equal Number of Points on Each Side of the Interface

N	Error in u	Error in v
8	1.57×10^{-2}	1.49×10^{-2}
16	4.15×10^{-6}	4.86×10^{-6}
32	1.91×10^{-9}	1.91×10^{-9}

Table VI. Effect of Streamwise Mesh Distribution on Ringleb Calculation

Grid	Division	Maximum Error
8 + 8	0.45 + 0.55	7.8×10^{-4}
8 + 8	0.50 + 0.50	9.3×10^{-4}
16 (SD)	-	1.9×10^{-3}
10 + 6	0.34 + 0.66	1.2×10^{-2}

NASA
National Aeronautics and Space Administration

Report Documentation Page

1. Report No.	2. Government Accession No.	3. Recipient's Catalog No.
NASA CR-178373 ICASE Report No. 87-62		

4. Title and Subtitle	5. Report Date
SPECTRAL COLLOCATION METHODS	September 1987
	6. Performing Organization Code

7. Author(s)	8. Performing Organization Report No.
M. Y. Hussaini, D. A. Kopriva, A. T. Patera	87-62
	10. Work Unit No. 505-90-21-01

9. Performing Organization Name and Address	11. Contract or Grant No.
Institute for Computer Applications in Science and Engineering Mail Stop 132C, NASA Langley Research Center Hampton, VA 23665-5225	NAS1-18107
	13. Type of Report and Period Covered
12. Sponsoring Agency Name and Address	Contractor Report
National Aeronautics and Space Administration Langley Research Center Hampton, VA 23665-5225	14. Sponsoring Agency Code

15. Supplementary Notes

Langley Technical Monitor:
Richard W. Barnwell

Final Report

Submitted to IMACS J. Numer. Anal.

16. Abstract

This review covers the theory and application of spectral collocation methods. Section 1 describes the fundamentals, and summarizes results pertaining to spectral approximations of functions. Some stability and convergence results are presented for simple elliptic, parabolic and hyperbolic equations. Applications of these methods to fluid dynamics problems are discussed in Section 2.

17. Key Words (Suggested by Author(s))	18. Distribution Statement
spectral methods, Navier-Stokes equations	34 - Fluid Mechanics and Heat Transfer 64 - Numerical Analysis Unclassified - unlimited

19. Security Classif. (of this report)	20. Security Classif. (of this page)	21. No. of pages	22. Price
Unclassified	Unclassified	70	A04